

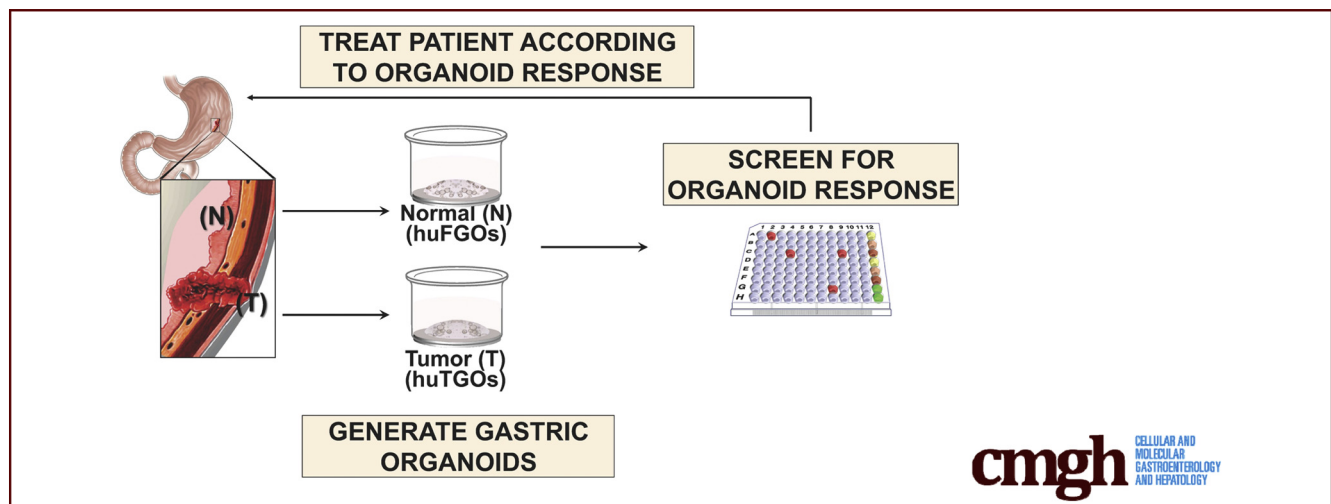
ORIGINAL RESEARCH

An Organoid-Based Preclinical Model of Human Gastric Cancer



Nina G. Steele,¹ Jayati Chakrabarti,² Jiang Wang,³ Jacek Biesiada,⁶ Loryn Holokai,⁴ Julie Chang,⁵ Lauren M. Nowacki,⁷ Jennifer Hawkins,⁸ Maxime Mahe,⁸ Nambirajan Sundaram,⁸ Noah Shroyer,⁷ Mario Medvedovic,⁶ Michael Helmrath,⁸ Syed Ahmad,⁹ and Yana Zavros³

¹Department of Cell and Developmental Biology, University of Michigan, Ann Arbor, Michigan; ²Department of Pharmacology and Systems Physiology, University of Cincinnati, Cincinnati, Ohio; ³Department of Pathology and Lab Medicine, University of Cincinnati College of Medicine, Cincinnati, Ohio; ⁴Department of Molecular Genetics, Biochemistry, and Microbiology, University of Cincinnati, Cincinnati, Ohio; ⁵Department of Biomedical Engineering, University of Cincinnati, Cincinnati, Ohio; ⁶Department of Environmental Health, Division of Biostatistics and Bioinformatics, University of Cincinnati College of Medicine, Cincinnati, Ohio; ⁷Department of Medicine, Section of Gastroenterology and Hepatology, Baylor College of Medicine, Houston, Texas; ⁸Department of Pediatric Surgery, Cincinnati Children's Hospital Medical Center, Cincinnati, Ohio; and ⁹Department of Surgery, University of Cincinnati Cancer Institute, Cincinnati, Ohio



SUMMARY

This study tests the potential of gastric cancer-derived organoids as an approach to predict *in vivo* tumor responses. Effect of standard-of-care therapies on organoids was correlated with results of *in vivo* treatment. The data suggest that patient-derived organoids will be useful in developing individualized therapies.

BACKGROUND & AIMS: Our goal was to develop an initial study for the proof of concept whereby gastric cancer organoids are used as an approach to predict the tumor response in individual patients.

METHODS: Organoids were derived from resected gastric cancer tumors (huTGOs) or normal stomach tissue collected from sleeve gastrectomies (huFGOs). Organoid cultures were treated with standard-of-care chemotherapeutic drugs corresponding to patient treatment: epirubicin, oxaliplatin, and 5-fluorouracil. Organoid response to chemotherapeutic

treatment was correlated with the tumor response in each patient from whom the huTGOs were derived. HuTGOs were orthotopically transplanted into the gastric mucosa of NOD scid gamma mice.

RESULTS: Whereas huFGOs exhibited a half maximal inhibitory concentration that was similar among organoid lines, divergent responses and varying half maximal inhibitory concentration values among the huTGO lines were observed in response to chemotherapeutic drugs. HuTGOs that were sensitive to treatment were derived from a patient with a near complete tumor response to chemotherapy. However, organoids resistant to treatment were derived from patients who exhibited no response to chemotherapy. Orthotropic transplantation of organoids resulted in the engraftment and development of human adenocarcinoma. RNA sequencing revealed that huTGOs closely resembled the patient's native tumor tissue and not commonly used gastric cancer cell lines and cell lines derived from the organoid cultures.

CONCLUSIONS: The treatment of patient-derived organoids alongside patients from whom cultures were derived will

ultimately test their usefulness to predict individual therapy response and patient outcome. (*Cell Mol Gastroenterol Hepatol* 2019;7:161-184; <https://doi.org/10.1016/j.jcmgh.2018.09.008>)

Keywords: Stomach; Organoids; Gastroids; Chemotherapy.

Gastric cancer is the fifth most common cancer worldwide and the third leading cause of cancer-related deaths, with a 5-year survival rate of only 29%.¹ The incidence of gastric cancer is 4 times more common in Japan than in the United Kingdom and United States and occurs at a younger age.² Because of the poor response of gastric cancer to various existing treatments, there is a need for approaches to predict the efficacy of therapy for individuals. We report here the generation of patient-derived gastric cancer organoids that may be useful for the prediction of patient responses to chemotherapy treatment.

Randomized data have clearly established that surgery alone for the treatment of gastric cancer results in reduced survival and increased recurrence rates when compared with multimodality therapy.¹ A current limitation for the treatment of gastric cancer is the lack of a reliable approach to identify which treatment options are most effective for each individual patient. For example, human epidermal growth factor receptor 2 (HER2) expression is used as a biomarker for the prediction of response to anti-HER2 monoclonal antibody trastuzumab in patients with metastatic gastric cancer.³ Currently, HER2 expression is determined by immunohistochemistry or by the detection of HER2 gene amplification by fluorescence in situ hybridization.^{4,5} However, because of tumor heterogeneity these approaches may represent inaccuracy in HER2 testing.⁶ Thus, further approaches are required to improve reliability of HER2 testing to ensure that patients receive the appropriate therapy for their individual disease.

Although cancer cell lines have proven valuable in the investigation of fundamental cancer research mechanisms, these models have the significant disadvantage of bearing little resemblance to the intended patient tumor.⁷⁻¹¹ The development of high-throughput analytical methods now enables us to address the clinical relevance of these human cancer-derived cell lines. At the genomic level, driver mutations may be retained within cancer cell lines. However, several studies reveal a drift at the transcriptomic level, demonstrating that cancer cell lines carry more resemblance to each other rather than to the clinical samples from which they were originally derived.^{9,10} Our study reports the use of three-dimensional organoids as a potential tool used for the prediction of targeted therapies for gastric cancer patients.

Results


Individual Patient-Derived Gastric Cancer Organoids Display Unique Responses to Chemotherapeutic Drugs and Targeted Therapy

We generated an initial bank of gastric cancer organoids from tumors obtained from 7 patients (Table 1). For each patient from whom the organoids were derived, patient

treatment, cancer staging, and tumor response and recurrence were recorded when available (Table 1). The morphology of each patient-derived organoid line (huTGO) was unique (Figure 1A and B). Specifically, we observed that whereas huTGO1 and 2 appeared as spherical nests with a central lumen lined by multiple layers of cells, huTGO4 exhibited a cribriform glandular morphology with cells forming multiple lumens of varying sizes (Figure 1A and B). HuTGO5 formed large spheres that consisted of a single epithelial layer by H&E staining (Figure 1A and B). All huTGO lines were passaged and re-formed organoids efficiently except for the huTGO3 line that lasted for only 4 passages before the line no longer persisted. Thus, we were unable to study the huTGO3 in the drug response assays. The proliferative response of each huTGO was measured by 5-ethynyl-2-deoxyuridine (EdU) uptake. This analysis revealed a divergent and significantly different proliferative rate among the different organoid lines (Figure 1C and D). In contrast to the huTGOs, normal human-derived normal fundic gastric organoid (huFGO) lines displayed similar morphologies both in culture (Figure 2A) and by H&E staining (Figure 2B). In addition, the proliferative rates of the huFGOs were not statistically different among the different organoid lines (Figure 2C and D).

To investigate whether huTGOs are a potential in vitro platform to study the efficacy of standard-of-care chemotherapeutic agents, organoids were treated with drugs that gastric cancer patients are typically treated with (epirubicin, oxaliplatin, 5-fluorouracil [5-FU]) (Figure 3A-C). As a comparison, organoids generated from normal gastric tissue (huFGOs) were treated with the same drugs (Figure 3D-F). In the huFGO lines it was observed that the half maximal inhibitory concentration (IC₅₀) values, as documented by an MTS cell viability assay, were similar among the organoid lines for each drug that was tested (Figure 3D-F). Statistical analysis revealed an overlapping 95% confidence interval between each huFGO line (Figure 4D-F), thus demonstrating that the IC₅₀ concentrations were not statistically different among these organoids. However, cell viability assays documented divergent responses and varying IC₅₀ values to drug treatments among the huTGO lines (Figure 3A-C, Figure 4A-C). Note that a shift of the curve to the right indicates a higher IC₅₀ (ie, more resistant to that particular drug). Cell viability assays were normalized to vehicle-treated controls to ensure that toxicity was specific to the drug effects.

Abbreviations used in this paper: CK, cytokeratin; DPBS, Dulbecco phosphate-buffered saline; EdU, 5-ethynyl-2'-deoxyuridine; 5-FU, 5-fluorouracil; HER2, human epidermal growth factor receptor 2; huFGO, human-derived normal fundic gastric organoid; huTGO, human-derived tumor gastric organoid; IC₅₀, half maximal inhibitory concentration; PD-L1, programmed death-ligand 1.

 Most current article

© 2019 The Authors. Published by Elsevier Inc. on behalf of the AGA Institute. This is an open access article under the CC BY-NC-ND license (<http://creativecommons.org/licenses/by-nc-nd/4.0/>).

2352-345X

<https://doi.org/10.1016/j.jcmgh.2018.09.008>

Table 1. Histologic Classification, Tumor Response, Number of Cases, and Organoid Lines Derived From Patients With Gastric Cancer

Histologic classification	No. of cases	Organoid line	Patient treatment and tumor response
Diffuse/intestinal	1	1: huTGO1	EOX, T3N1M1, no evaluation of tumor response
Diffuse	3	1: huTGO3 (Baylor) 2: No cell growth 3: huTGO6	Unknown Unknown No chemo, T2N3aM1, no evaluation of tumor response
Intestinal	3	1: huTGO2 2: huTGO5 3: huTGO7	No chemo, T1bN0M0, no evaluation of tumor response EOX, T3N0M0, no response to EOX (grade 3) EOX, T3N3M0, complete response (grade 1)
Signet-ring cell	2	1: No cell growth 2: No cell growth	Unknown Unknown
Poorly differentiated adenocarcinoma with diffuse and signet-ring patterns	1	1: huTGO4	EOX, T4N3M0, no response to EOX (grade 3)

NOTE. Based on the criteria by the College of American Pathologists: grade 1: complete (0% residual tumor; grade 1a) or subtotal tumor regression (10% residual tumor per tumor bed; grade 1b); grade 2, partial tumor regression (10%–50% residual tumor per tumor bed); and grade 3, minimal or no tumor regression (50% residual tumor per tumor bed) (Becker et al, Cancer 2003;98:1521–1530).

We wanted to next correlate the drug response of each huTGO line to the corresponding patient's tumor response from whom the cultures were derived. Lines huTGO1, huTGO2, and huTGO6 were among the more resistant to chemotherapeutic drug treatment. Resistance was documented on the basis of decreased percentage of dead cells in organoid response to combination treatment with epirubicin, oxaliplatin, and 5-FU through the use of a fluorescence-based live/dead cell viability assay (Figure 5A and C). Unfortunately, evaluation of tumor response in these patients was not performed (Table 1). This is because (1) the patient from whom huTGO1 organoids were derived exhibited metastatic gastric cancer and the tumor was not resected, and (2) the patients from whom huTGO2 and huTGO6 organoids were derived did not receive chemotherapy and therefore tumor response was not evaluated (Table 1). The huTGO4 line displayed decreased resistance in response to chemotherapeutic drug treatment; however, this particular patient did not respond to chemotherapy (Table 1). Also, compared with huTGO1, 2, and 6, huTGO4 responded partially to the combination in vitro treatment of the organoids as documented by the significant increase in the percent of dead cells within the organoid cultures within 48 hours of treatment (Figure 5A). However, huTGO7 was highly responsive to drug treatment, and similarly the patient's tumor exhibited a near complete response to the same chemotherapy combination therapy (Table 1, Figure 5A and D). Importantly, whereas the huTGO lines exhibited differences in the response to drug treatment, huFGOs showed similar response to the combination drug treatment (Figure 5B). We were unable to perform a similar analysis on huTGO5 because this culture did not persist. Our studies suggest that each organoid line may be useful to help determine an active chemotherapeutic drug(s) for patient treatment. However, just as important is our ability to define drugs for which a patient has a resistance and

may predominantly be causing side effects with little therapeutic response.

We observed that the huTGO1 and huTGO2 organoid lines expressed HER2, whereas huTGO4 and huTGO6 did not express this protein (Figure 6A). This observation was contradictory to the pathologist's observations of the tumor tissue that reported all patients to be negative for HER2. The patient from whom huTGO1 was derived did not undergo tumor resection, but rather HER2 status was determined on the basis of tissue collected from the metastatic tumor. We tested whether HER2 inhibition sensitized the huTGOs to epirubicin, oxaliplatin, and 5-FU treatment (Figure 6B–E). For example, huTGO1 was most resistant to epirubicin (IC₅₀, 17.66 ± 0.09), oxaliplatin (IC₅₀, 31.57 ± 0.06), and 5-FU (IC₅₀, 13.88 ± 0.07) (Figure 6B, Figure 7). However, when huTGO1s were pretreated with HER2 inhibitor, the IC₅₀ decreased to 6.05 ± 0.06, 7.93 ± 0.05, and 7.25 ± 0.05 in response to epirubicin, oxaliplatin, and 5-FU, respectively (Figure 6B, Figure 7). Similarly, pretreatment of huTGO2s with HER2 inhibitor also sensitized the organoids to epirubicin (IC₅₀ epirubicin, 98.8 ± 0.09; IC₅₀ epirubicin + HER2I, 3.19 ± 0.10), oxaliplatin (IC₅₀ oxaliplatin, 17.09 ± 0.04; IC₅₀ oxaliplatin + HER2I, 1.74 ± 0.07), and 5-FU (IC₅₀ 5-FU, 25.13 ± 0.05; IC₅₀ 5-FU + HER2I, 2.34 ± 0.06) (Figure 6C, Figure 8). The huTGO4 and 6 lines did not express HER2 (Figure 6A) and were not responsive to HER2 inhibitor pretreatment (Figure 6D and E, Figures 9 and 10). It is important to note that Mubritinib specifically inhibits the tyrosine kinase activity of HER2 signaling and cannot reproduce the effects that trastuzumab has on host immune surveillance.¹² Including the patient's immune cell in an organoid co-culture is part of our future plans. Thus, we may propose that on the basis of our observations, patient-derived gastric cancer organoids may serve as a platform for testing the efficacy of targeted therapies in individual patients.

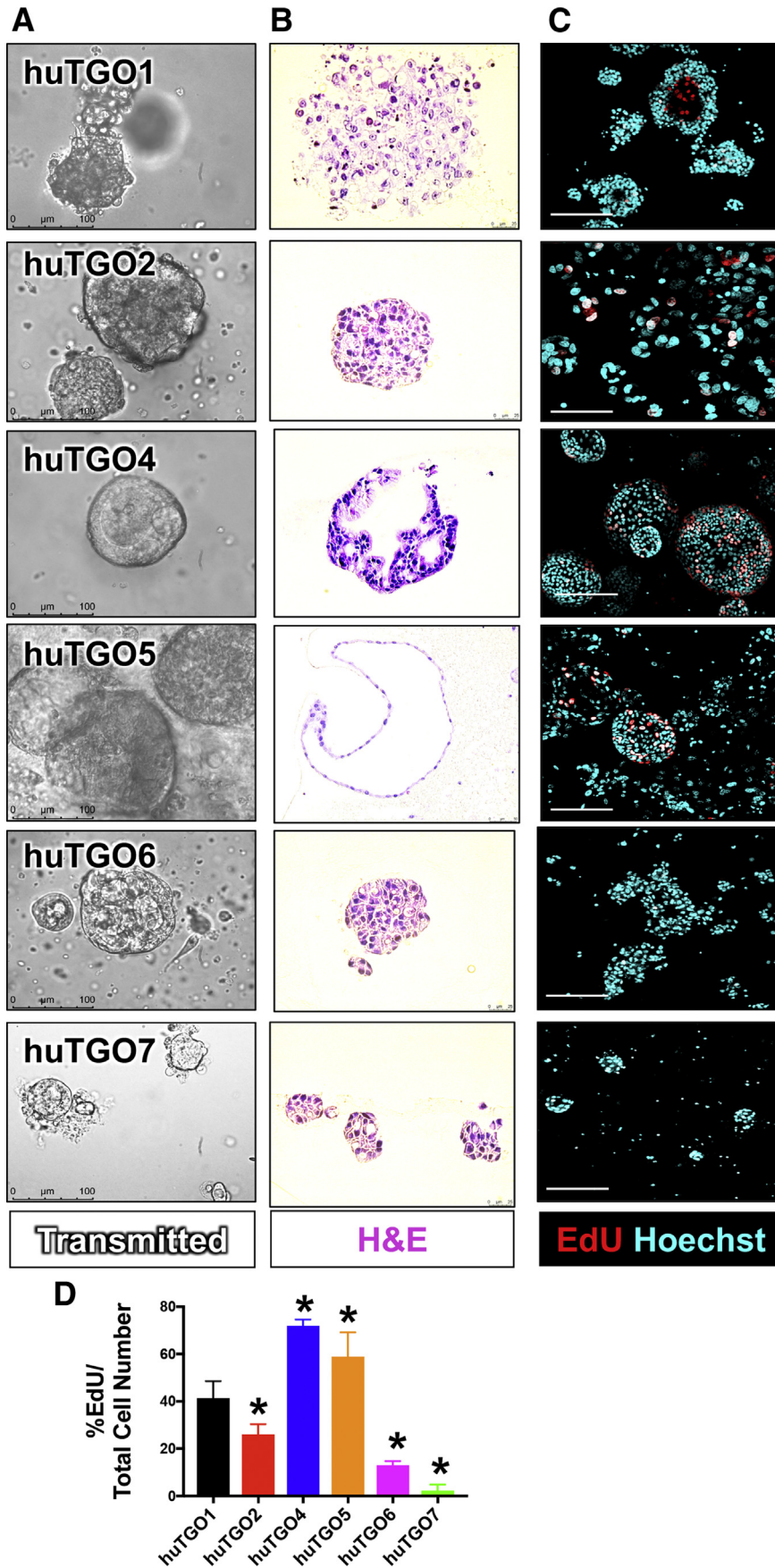


Figure 1. Morphologic differences and proliferative rate of patient-derived gastric cancer organoids (huTGOs). (A) Light micrographs of patient-derived gastric cancer organoid lines. (B) H&E staining of gastric cancer organoids. (C) Proliferation of huTGO lines as measured by EdU (red) uptake (Hoechst, cyan). (D) Quantification of proliferation as measured by %EdU expressing cells/total cell number in huTGOs. * $P < .05$ compared with huTGO1; $n = 6$ individual organoids were quantified per line.

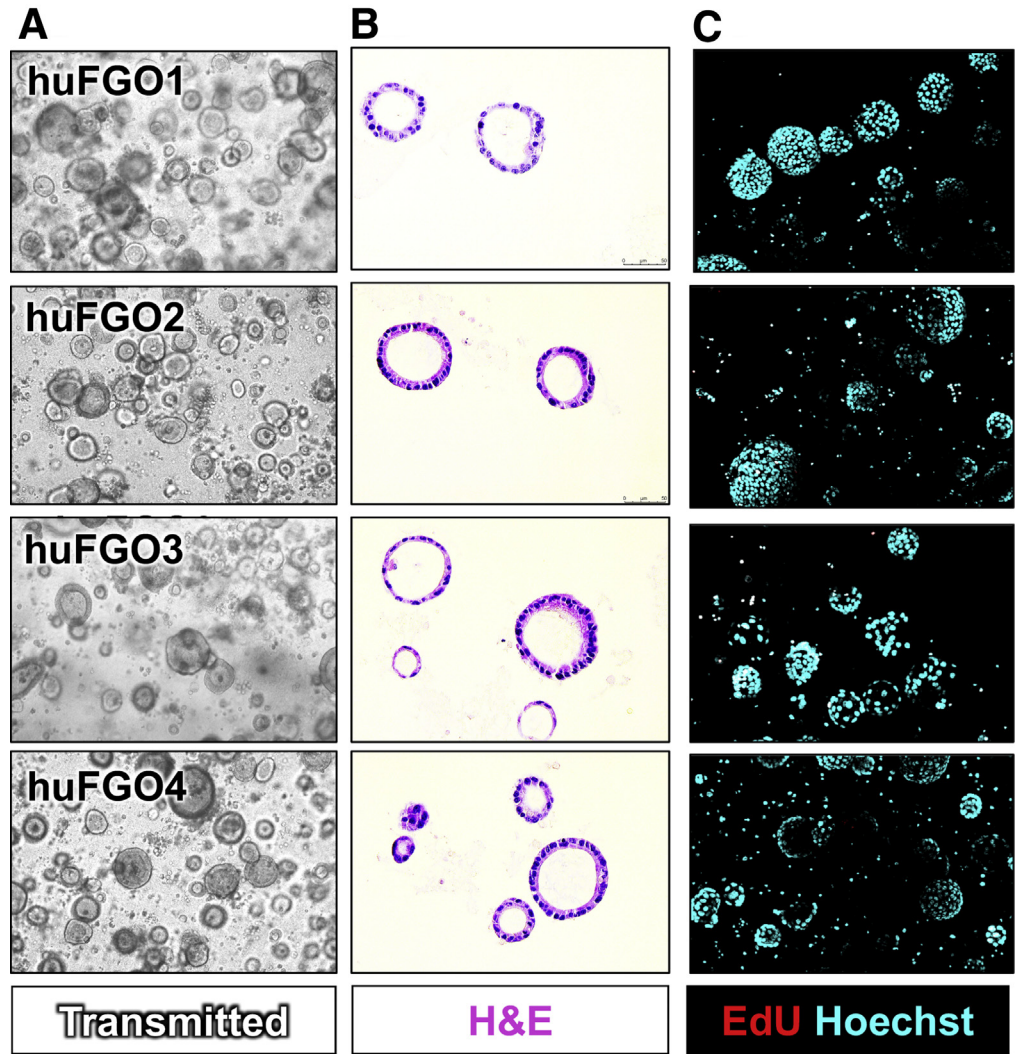
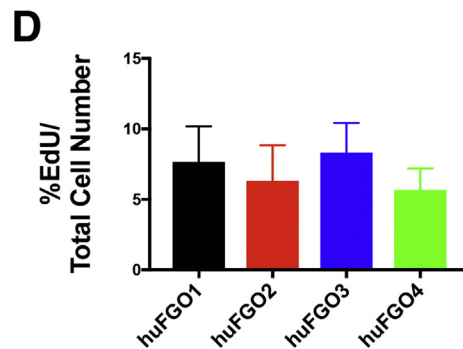


Figure 2. Morphologic differences and proliferative rate of patient-derived gastric organoids (huFGOs). (A) Light micrographs of patient-derived gastric organoid lines. (B) H&E staining of gastric organoids. (C) Proliferation of huFGO lines as measured by EdU (red) uptake (Hoechst, cyan). (D) Quantification of proliferation as measured by % EdU expressing cells/total cell number in huFGOs. * $P < .05$ compared with huTGO1; $n = 6$ individual organoids were quantified per line.



Patient-Derived Gastric Cancer Organoids Phenotypically Resemble the Native Tumor Tissue

In support of carcinogenesis, these cultures also rapidly developed tumors in an in vivo xenograft mouse model (Figure 11A). We questioned the extent to which huTGOs

recapitulate their original tumor histology in vivo. HuTGO1 and 2 were xenotransplanted subcutaneously into NSG mice (Figure 11B and C). Notably, histologic and differentiation patterns of the patient tumor tissue were highly recapitulated in the xenograft tumors established from the

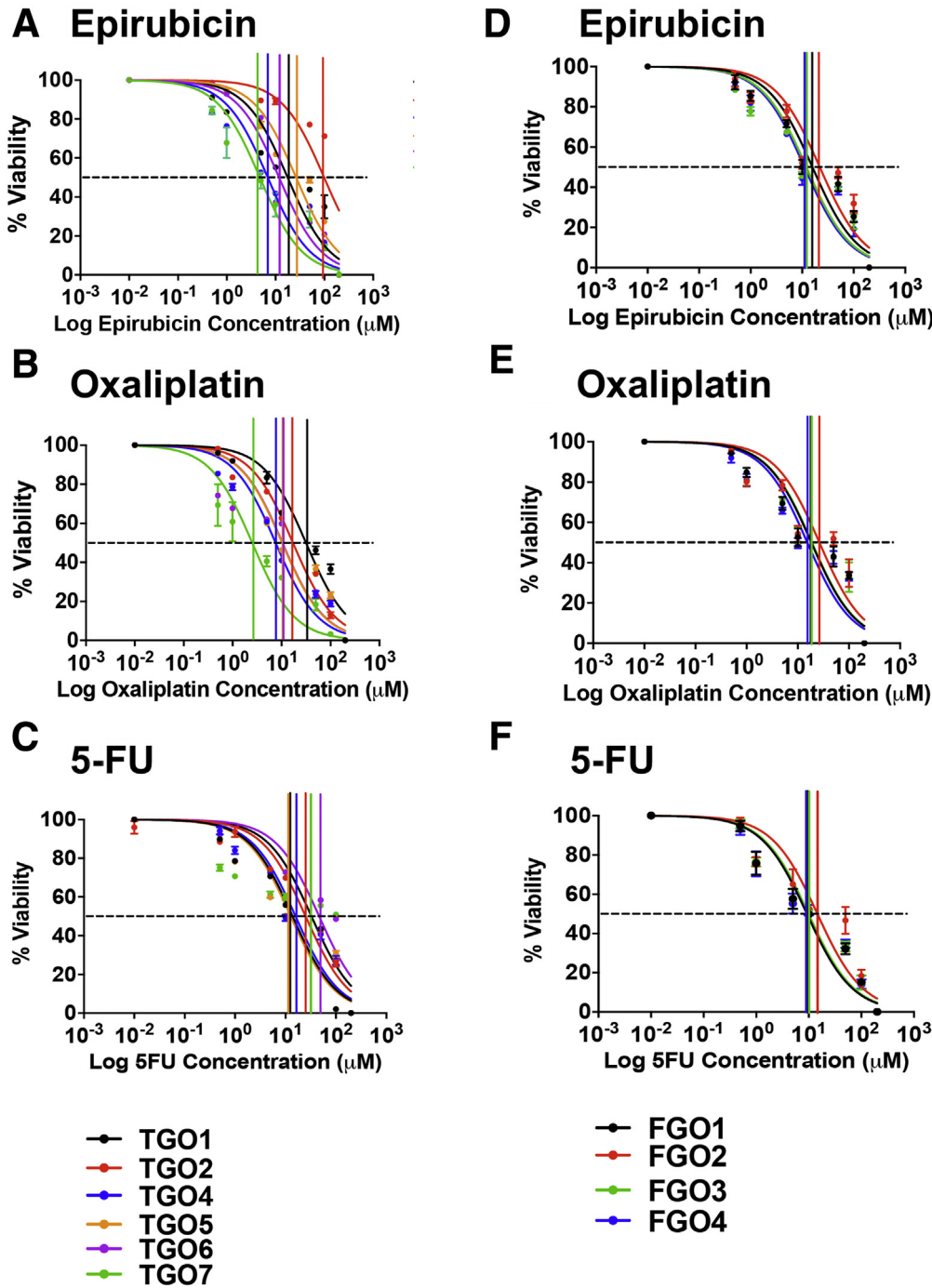


Figure 3. Drug responses of patient-derived gastric cancer and normal organoids. Dose-response curves generated from patient-derived (A–C) gastric cancer (huTGO) and (D–F) normal (huFGO) organoid lines treated with epirubicin, oxaliplatin, or 5-FU. These plots demonstrate the percent of viable cells as measured by an MTS assay in response to micromolar doses of chemotherapeutic agents. Each assay was run in triplicate for each individual organoid line.

organoids (Figure 11B and C). For example, huTGO2 derived from well-differentiated intestinal-type gastric adenocarcinoma is composed of glandular structures (Figure 11C, PDX-huTGO2) and is similar to patient’s specimen (Figure 11C, P-huTGO2). Organoids derived from mixed poorly differentiated diffuse and intestinal-type gastric cancer tissues (huTGO1) formed similar morphologies in vivo including infiltrating single tumor cells (diffuse-type) and adjacent cancer glands (intestinal-type) (Figure 11B, PDX-huTGO1).

Patient-Derived Gastric Cancer Organoids Engraft Within the Gastric Epithelium of a Mouse and Form Adenocarcinoma

Investigating the impact of the endogenous environment of the stomach on tumor growth is part of our future research plans. Thus, we sought to develop an orthotopic transplantation model using patient-derived gastric cancer organoids. HuTGO1 and 2 organoid lines were transplanted

A Epirubicin - huTGOs

log(inhibitor) vs. normalized response	TGO1	TGO2	TGO4	TGO5	TGO6	TGO7
LogIC50	1.247 ± 0.09	1.995 ± 0.09	0.8403 ± 0.07	1.421 ± 0.06	1.072 ± 0.06	0.6774 ± 0.08
IC50	17.66 ± 0.09	98.81 ± 0.09	6.923 ± 0.07	26.36 ± 0.06	11.8 ± 0.06	4.758 ± 0.08
95% CI (profile likelihood)						
LogIC50	1.021 to 1.473	1.819 to 2.172	0.6708 to 1.011	1.294 to 1.544	0.9509 to 1.196	0.4932 to 0.858
IC50	10.5 to 29.7	65.88 to 148.5	4.686 to 10.25	19.67 to 35.03	8.932 to 15.69	3.113 to 7.214

B Oxaliplatin - huTGOs

log(inhibitor) vs. normalized response	TGO1	TGO2	TGO4	TGO5	TGO6	TGO7
LogIC50	1.499 ± 0.06	1.233 ± 0.04	0.8786 ± 0.05	1.011 ± 0.07	1.019 ± 0.09	0.4004 ± 0.08
IC50	31.57 ± 0.06	17.09 ± 0.04	7.561 ± 0.05	10.25 ± 0.07	10.45 ± 0.09	2.514 ± 0.08
95% CI (profile likelihood)						
LogIC50	1.372 to 1.622	1.15 to 1.316	0.7649 to 0.992	0.8484 to 1.178	0.8063 to 1.229	0.1918 to 0.6057
IC50	23.54 to 41.91	14.11 to 20.69	5.82 to 9.826	7.053 to 15.07	6.402 to 16.94	1.555 to 4.034

C 5-FU - huTGOs

log(inhibitor) vs. normalized response	TGO1	TGO2	TGO4	TGO5	TGO6	TGO7
LogIC50	1.142 ± 0.07	1.4 ± 0.05	1.2 ± 0.07	1.1 ± 0.09	1.7 ± 0.09	1.5 ± 0.13
IC50	13.88 ± 0.07	25.13 ± 0.05	15.87 ± 0.07	12.73 ± 0.09	46.7 ± 0.09	32.7 ± 0.13
95% CI (profile likelihood)						
LogIC50	0.9823 to 1.302	1.284 to 1.513	1.037 to 1.366	0.8853 to 1.333	1.465 to 1.857	1.099 to 1.847
IC50	9.601 to 20.04	19.24 to 32.61	10.89 to 23.24	7.678 to 21.52	29.18 to 71.9	12.55 to 70.32

D Epirubicin - huFGOs

log(inhibitor) vs. normalized response	FGO1	FGO2	FGO3	FGO4
LogIC50	1.199 ± 0.07	1.342 ± 0.08	1.083 ± 0.07	1.045 ± 0.06
IC50	15.83 ± 0.07	21.99 ± 0.08	12.09 ± 0.07	11.1 ± 0.06
95% CI (profile likelihood)				
LogIC50	1.041 to 1.36	1.154 to 1.526	0.9034 to 1.266	0.8945 to 1.2
IC50	11 to 22.89	14.26 to 33.56	8.005 to 18.47	7.843 to 15.85

E Oxaliplatin - huFGOs

log(inhibitor) vs. normalized response	FGO1	FGO2	FGO3	FGO4
LogIC50	1.264 ± 0.08	1.422 ± 0.09	1.276 ± 0.08	1.186 ± 0.08
IC50	18.38 ± 0.08	26.43 ± 0.09	18.87 ± 0.08	15.34 ± 0.08
95% CI (profile likelihood)				
LogIC50	1.071 to 1.458	1.207 to 1.625	1.082 to 1.468	0.9728 to 1.404
IC50	11.78 to 28.68	16.09 to 42.15	12.09 to 29.35	9.392 to 25.37

F 5-FU - huFGOs

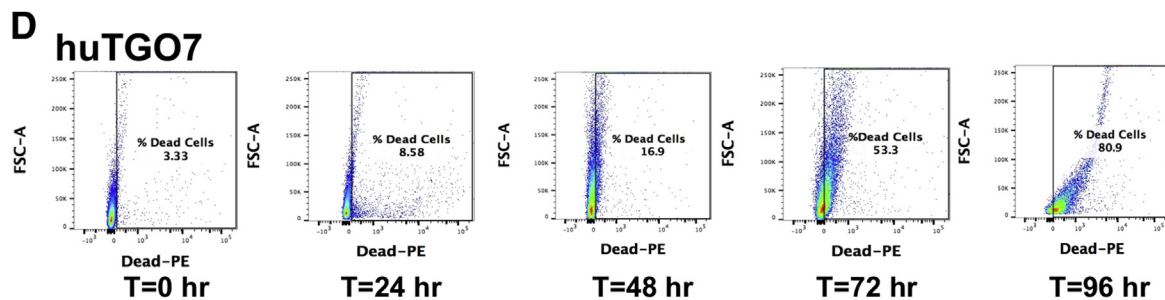
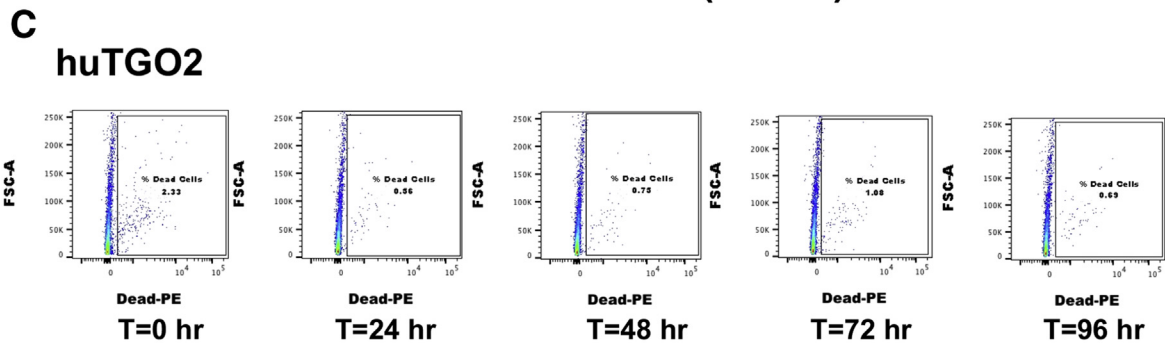
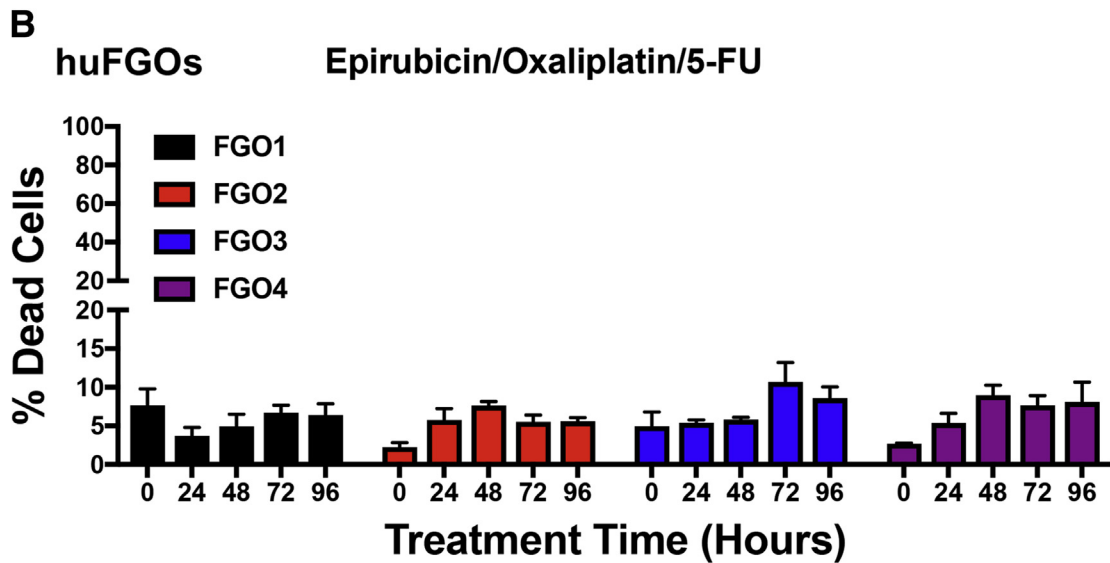
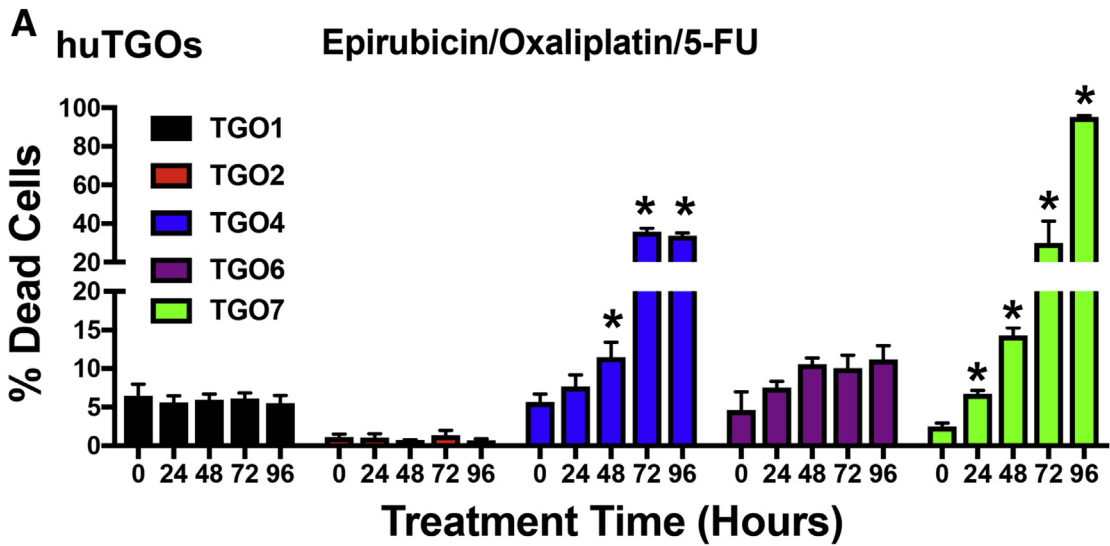
log(inhibitor) vs. normalized response	FGO1	FGO2	FGO3	FGO4
LogIC50	0.9655 ± 0.06	1.163 ± 0.08	0.9944 ± 0.06	0.9722 ± 0.07
IC50	9.237 ± 0.06	14.57 ± 0.08	9.872 ± 0.06	9.379 ± 0.07
95% CI (profile likelihood)				
LogIC50	0.8253 to 1.107	0.9642 to 1.365	0.8515 to 1.139	0.8132 to 1.133
IC50	6.687 to 12.8	9.209 to 23.16	7.104 to 13.77	6.504 to 13.59

Figure 4. IC50 values for huTGO and huFGO dose-response curves. IC50 values for tumor-derived gastric organoids (huTGO) treated with (A) epirubicin, (B) oxaliplatin, and (C) 5-FU. IC50 values for normal gastric tissue (huFGOs) treated with (D) epirubicin, (E) oxaliplatin, and (F) 5-FU. CI, confidence interval.

into the submucosa of the gastric epithelium of NSG mice (Figure 11D–F). After organoid transplantation we observed the development of adenocarcinoma with areas of cells invading the epithelium (Figure 11D–H). Of note, human cells were detected in areas of adenocarcinoma and the epithelium of the mouse gastric mucosa with the use of an

antibody specific for human histone protein (Figure 11H and J).

The expression of cytokeratin (CK) 7 and CK20 is often used for the diagnosis of gastric cancer. Immunohistochemical staining revealed high expression of CK7 within the lesions originating from the huTGO1 (Figure 12A) and



huTGO2 (Figure 12B) organoid orthotopic transplantations. In contrast, CK20 was only detected in the stomachs of mice transplanted with huTGO2 (Figure 12D) compared with those animals transplanted with huTGO1 (Figure 12C). Lesions arising from huTGO1 and huTGO2 were highly proliferative (Figure 12E and F). Expression of E-cadherin (Figure 12G and H) was also detected within these lesions of mice transplanted with huTGO1 and 2 organoids. The negative control for the human-specific histone immunofluorescence is shown in Figure 13. Collectively, these data suggest that transplantation of patient-derived gastric cancer organoids engraft within the gastric epithelium and mimic their parental histology.

Gastric Cancer Organoids Resemble the Patient's Tumor Tissue From Which They Are Derived

HuTGO1-7 organoid lines were able to grow efficiently without organoid media and rapidly formed cell lines. To test the dependence of normal (huFGOs, organoids derived from normal human gastric tissue) and tumor-derived gastric organoids (huTGOs) on key growth factors supplied in the organoid growth medium, organoids were dissociated to single cells and re-suspended in organoid media with or without the key growth factors. HuTGOs grew in a growth factor-independent manner relative to control organoids (Figure 14A and B).

RNA sequencing followed by patient-matched statistical analysis identified 251 genes differentially expressed between samples derived from organoids and tissue samples and samples derived from two-dimensional cultures (false discovery rate <0.1). Hierarchical clustering analysis of differentially expressed genes (Figure 15) and samples, including the samples from 2 commonly used gastric cancer cell lines (AGS and NCI-N87), revealed 3 major patterns of expression: genes down-regulated in two-dimensional cultures, genes up-regulated in two-dimensional cultures, and genes that were down-regulated in both TGO and two-dimensional cultures. Interestingly, genes down-regulated in both TGO and two-dimensional cultures were enriched by genes with several immune-response Gene Ontology categories (Table 2). This is consistent with the lack of the immune response within organoid and cell line cultures. Furthermore, gene expression profiles from AGS and NCI-N87 gastric cell lines were virtually identical to profiles of our two-dimensional cultures and different from TGO and cancer tissue samples, although these samples were not used in the selection of differentially expressed genes.

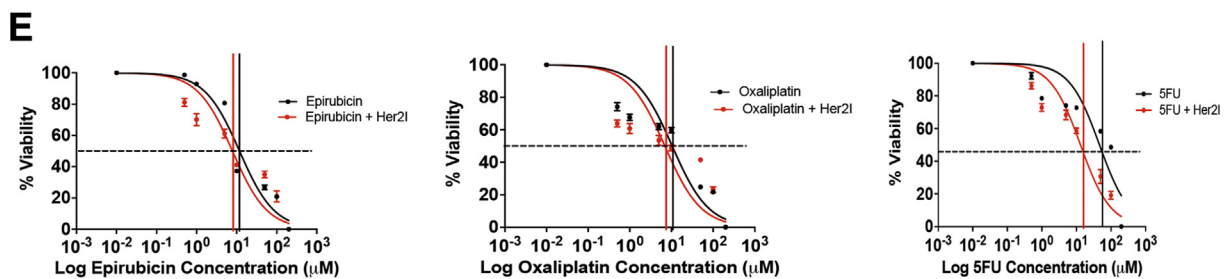
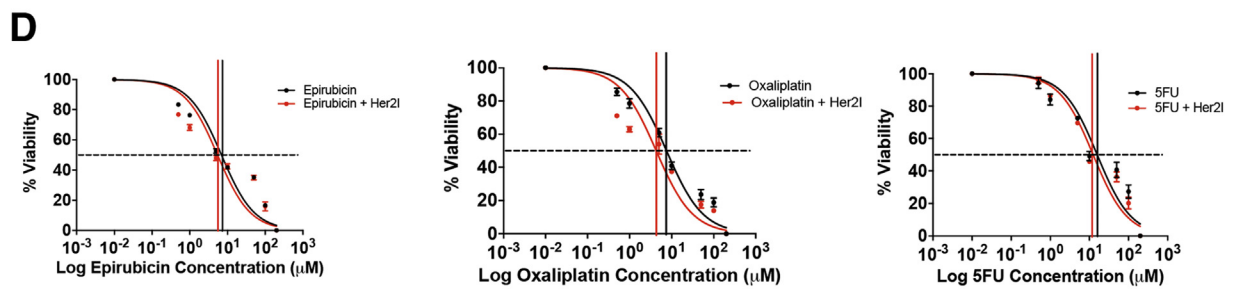
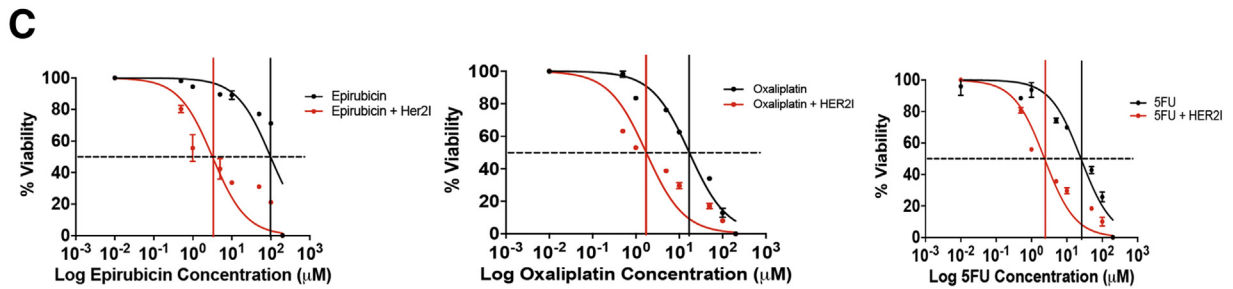
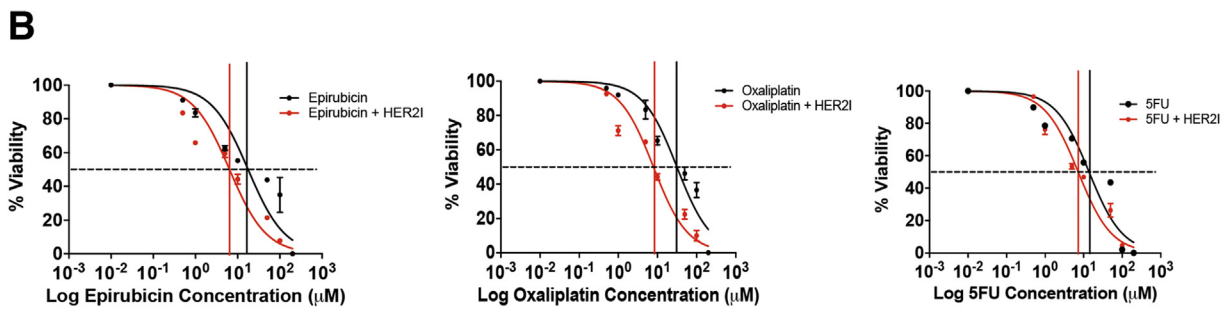
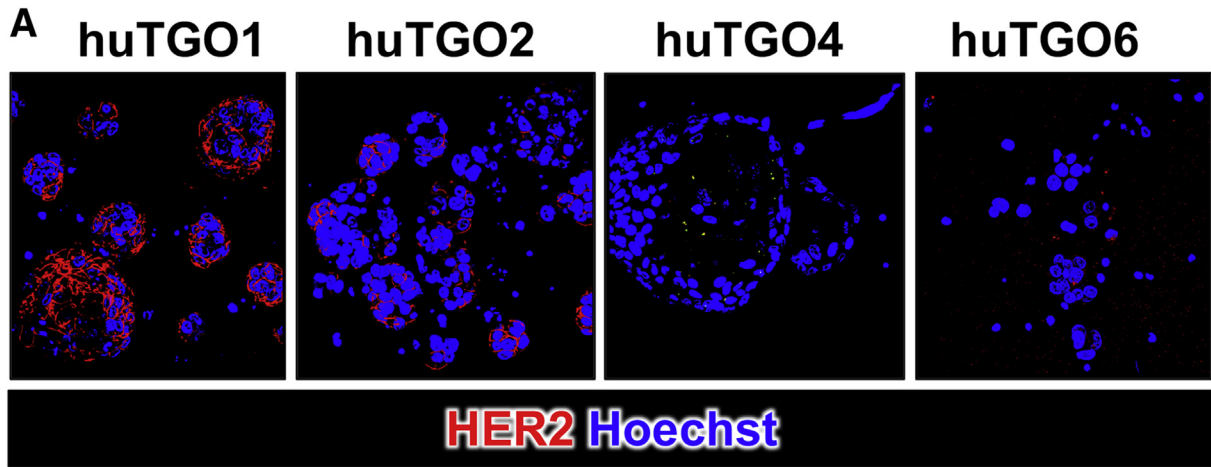
The genes that were highly expressed in gastric cancer tissue and organoids (TGOs) included GPD1, CXCR4, OLFM4, IL13R α 2, and carbonic anhydrase (CA9). Genes that were identified as being uniquely expressed in the cell lines

included KRT80, AMIGO2, CDKN2B, KRT23, and BAMBI. The expression of the genes among gastric cancer tissue 1, 2, 4, 5, and 7, TGO1, 2, 4, 5 and 7 lines, and cell lines was verified by quantitative real-time polymerase chain reaction (Figure 16). Collectively, these data suggest that gastric cancer organoids resemble the patient's tumor tissue from which they were derived.

Discussion

We demonstrate the proof of concept for the use of gastric cancer organoids as a preclinical model to potentially evaluate the efficacy of cancer therapeutics. The development of these organoid cultures represents the first step that is required to establish in vivo and in vitro patient-derived organoid-based platforms for personalized medicine. Cell lines have been the most frequently used models in cancer research, and their use has certainly advanced our understanding of cancer biology. As opposed to standard-of-care chemotherapeutic agents, targeted therapy is applied to the percentage of patients expressing a specific molecular abnormality. Thus, a large part of our ability to develop personalized medicine depends on cultures that capture this genetic heterogeneity. However, many studies report genomic differences between cancer cell lines and tissue samples from which they are derived.⁷⁻¹¹ On the basis of RNA sequencing data and hierarchical clustering, we document a phenotypical similarity between the organoids and the patient's tumor tissue. This is in stark contrast to a cell line derived from the gastric cancer organoids, which has a similar transcriptional program to that of the well-established gastric cancer cell lines AGS and NCI-N87 cells. Importantly, a limitation of the organoid and cell line cultures is the lack of the immune component that is found within the patient's tumor environment. These findings are of significance because tumors can evade immune surveillance by expressing molecules such as programmed death-ligand 1 (PD-L1) that interacts with PD-1 and subsequently inhibiting CD8⁺ cytotoxic T-lymphocyte proliferation, survival, and effector function.¹³⁻¹⁵ On average, PD-L1 expression is detected in approximately 42.2% of gastric adenocarcinomas.¹⁶ Although anti-PD1 antibodies are already in clinical trials for gastric cancer treatment,¹⁷⁻¹⁹ there are currently no preclinical models that allow us to test the efficacy of therapy to predict patient treatment response and outcome. Refining the organoid culture system to include the patient's own immune response would be beneficial to identifying the efficacy of immunotherapy in patients. Collectively, our data and published studies direct us toward developing in vitro models, such as the gastric cancer organoids, that would help to better predict the success or failure of chemotherapeutic agents and targeted therapies. Of importance, we have

Figure 5. (See previous page). Organoid responses to combined treatment with epirubicin, oxaliplatin, and 5-FU. Quantification of flow cytometric cell viability analysis at 0, 24, 48, 72, and 96 hours after treatment with combined epirubicin, oxaliplatin, and 5-FU of (A) huTGOs and (B) huFGOs. Representative flow cytometry dot plots at 0, 24, 48, 72, and 96 hours after treatment with combined epirubicin, oxaliplatin, and 5-FU in (C) huTGO2 and (D) huTGO7. * $P < .05$ compared with $t = 0$ hours. Each assay was run in triplicate for each individual organoid line.



A Epirubicin – huTGO1

log(inhibitor) vs. normalized response	Epirubicin	Epirubicin + HER2I
LogIC50	1.247 ± 0.09	0.8065 ± 0.06
IC50	17.66 ± 0.09	6.405 ± 0.06
95% CI (profile likelihood)		
LogIC50	1.021 to 1.473	0.6621 to 0.9477
IC50	10.5 to 29.7	4.593 to 8.866

B Oxaliplatin – huTGO1

log(inhibitor) vs. normalized response	Oxaliplatin	Oxaliplatin + HER2I
LogIC50	1.499 ± 0.06	0.8995 ± 0.05
IC50	31.57 ± 0.06	7.934 ± 0.05
95% CI (profile likelihood)		
LogIC50	1.372 to 1.622	0.79 to 1.009
IC50	23.54 to 41.91	6.166 to 10.2

C 5-FU – huTGO1

log(inhibitor) vs. normalized response	5FU	5FU + HER2I
LogIC50	1.142 ± 0.07	0.8603 ± 0.05
IC50	13.88 ± 0.07	7.249 ± 0.05
95% CI (profile likelihood)		
LogIC50	0.9823 to 1.302	0.7527 to 0.9678
IC50	9.601 to 20.04	5.658 to 9.286

Figure 7. IC50 values for huTGO1 dose-response curves. IC50 values for tumor-derived gastric organoids (huTGO) treated with (A) epirubicin with or without HER2I, (B) oxaliplatin with or without HER2I, or (C) 5-FU with or without HER2I. CI, confidence interval.

optimized these cultures such that organoids can be directly grown in a 96-well plate format and used for drug testing within 3 days of the patient's surgery. Thus, it is feasible to inform the clinician of possible treatment options within 5–6 days of surgery.

Investigating the impact of the endogenous environment of the stomach on tumor growth is an important direction of

our future research plans. An orthotopic transplantation model using patient-derived gastric cancer organoids was developed. Organoids that were transplanted into the submucosa below the gastric epithelium of NSG mouse stomachs developed into adenocarcinoma, and this was confirmed by a board-certified pathologist. The lesions were originated from human organoids as

Figure 6. (See previous page). HER2 expression and responsiveness to HER2 inhibition in patient-derived gastric cancer organoids. (A) Immunofluorescence of HER2 expression (red) in huTGOs. Dose-response curves generated by using (B) huTGO1, (C) huTGO2, (D) huTGO4, and (E) huTGO6 organoid lines in response to epirubicin, oxaliplatin, or 5-FU with or without HER2 inhibitor (HER2I). Each assay was run in triplicate for each individual organoid line.

A Epirubicin – huTGO2

log(inhibitor) vs. normalized response	Epirubicin	Epirubicin + HER2I
LogIC50	1.995 ± 0.09	0.5049 ± 0.1
IC50	98.81 ± 0.09	3.198 ± 0.1
95% CI (profile likelihood)		
LogIC50	1.819 to 2.172	0.2522 to 0.7538
IC50	65.88 to 148.5	1.787 to 5.673

B Oxaliplatin – huTGO2

log(inhibitor) vs. normalized response	Oxaliplatin	Oxaliplatin + HER2I
LogIC50	1.233 ± 0.04	0.2397 ± 0.07
IC50	17.09 ± 0.04	1.737 ± 0.07
95% CI (profile likelihood)		
LogIC50	1.15 to 1.316	0.04842 to 0.4364
IC50	14.11 to 20.69	1.118 to 2.732

C 5-FU – huTGO2

log(inhibitor) vs. normalized response	5FU	5FU + HER2I
LogIC50	1.4 ± 0.05	0.3695 ± 0.06
IC50	25.13 ± 0.05	2.341 ± 0.06
95% CI (profile likelihood)		
LogIC50	1.284 to 1.513	0.2287 to 0.5108
IC50	19.24 to 32.61	1.693 to 3.242

Figure 8. IC50 values for huTGO2 dose-response curves. IC50 values for tumor-derived gastric organoids (huTGO) treated with (A) epirubicin with or without HER2I, (B) oxaliplatin with or without HER2I, or (C) 5-FU with or without HER2I. CI, confidence interval.

documented by the positive immunostaining using anti-human histone antibody. Organoid-derived lesions were highly proliferative, and huTGO1 and huTGO2 differentially expressed CK7 and CK20. The expressions of CK7 and CK20 are often used as prognostic markers for gastric cancer.²⁰ Cytokeratin (CK), an intermediate filament that is expressed in epithelial cells, plays an important role as a cytoskeletal component in the maintenance of cell morphology. The CK gene has 20 subtypes, and the expression of CK depends primarily on the epithelial cell type and the degree of differentiation.²¹ Early studies report that the expression of CK7 and/or CK20 showed a tendency

toward a high positive rate in the differentiated type of gastric cancer.²⁰ Our data showed that whereas CK7 was highly expressed in lesions arising from the transplant of TGO1 and 2 organoid lines, CK20 was not expressed in TGO1-derived transplants. This is significant because TGO1 was an organoid line derived from a patient with a mixed, poorly differentiated, and intestinal-type gastric cancer. In support of our studies, a recent study demonstrated the development of an orthotopic mouse model whereby gastric cancer cell lines tagged with luciferase and injected into the subserosa of the stomach allows for monitoring of primary tumor growth and metastasis in real-time.²² Our RNA

A Epirubicin – huTGO4

log(inhibitor) vs. normalized response	Epirubicin	Epirubicin + HER2I
LogIC50	0.8403 ± 0.07	0.7355 ± 0.09
IC50	6.923 ± 0.07	5.438 ± 0.09
95% CI (profile likelihood)		
LogIC50	0.6708 to 1.01	0.5127 to 0.9537
IC50	4.686 to 10.25	3.256 to 8.989

B Oxaliplatin – huTGO4

log(inhibitor) vs. normalized response	Oxaliplatin	Oxaliplatin + HER2I
LogIC50	0.8786 ± 0.05	0.633 ± 0.08
IC50	7.561 ± 0.05	4.295 ± 0.08
95% CI (profile likelihood)		
LogIC50	0.7649 to 0.992	0.4366 to 0.819
IC50	5.82 to 9.826	2.733 to 6.591

C 5-FU – huTGO4

log(inhibitor) vs. normalized response	5FU	5FU + HER2I
LogIC50	1.2 ± 0.07	1.096 ± 0.06
IC50	15.87 ± 0.07	12.48 ± 0.06
95% CI (profile likelihood)		
LogIC50	1.037 to 1.366	0.971 to 1.224
IC50	10.89 to 23.24	9.354 to 16.74

Figure 9. IC50 values for huTGO4 dose-response curves. IC50 values for tumor-derived gastric organoids (huTGO) treated with (A) epirubicin with or without HER2I, (B) oxaliplatin with or without HER2I, or (C) 5-FU with or without HER2I. CI, confidence interval.

sequencing data suggest that the use of gastric cancer cell lines may be a limitation because the patient-derived organoids express a transcriptional profile more similar to the patient's primary tumor tissue than the profile of gastric cancer cell lines. Thus, we advance these recent studies by demonstrating that orthotopic transplantation of cancer-derived organoid lines is clinically relevant and may recapitulate tumor growth and metastasis in vivo.

The current work supports the finding that cancer organoids derived from resected gastric cancer tumors may

capture the response to standard-of-care chemotherapeutics of the patient's native tumor. Our data showed that each huTGO line exhibited a unique response to epirubicin, oxaliplatin, and 5-FU, when compared with the non-divergent responses of huFGOs to the same drugs. These results may be attributed to the heterogeneity in each cancer organoid line exhibiting various mutations that do not exist in organoids derived from normal tissue. A recent study also reporting the development of gastric cancer organoids supports our findings.²³ Seidlitz et al²³ report

A Epirubicin – huTGO6

log(inhibitor) vs. normalized response	Epirubicin	Epirubicin + HER2I
LogIC50	1.072 ± 0.06	0.8955 ± 0.08
IC50	11.8 ± 0.06	7.862 ± 0.08
95% CI (profile likelihood)		
LogIC50	0.9509 to 1.196	0.6932 to 1.099
IC50	8.932 to 15.69	4.934 to 12.57

B Oxaliplatin – huTGO6

log(inhibitor) vs. normalized response	Oxaliplatin	Oxaliplatin + HER2I
LogIC50	1.019 ± 0.09	0.8421 ± 0.1
IC50	10.45 ± 0.09	6.952 ± 0.1
95% CI (profile likelihood)		
LogIC50	0.8063 to 1.225	0.461 to 1.205
IC50	6.402 to 16.94	2.891 to 16.05

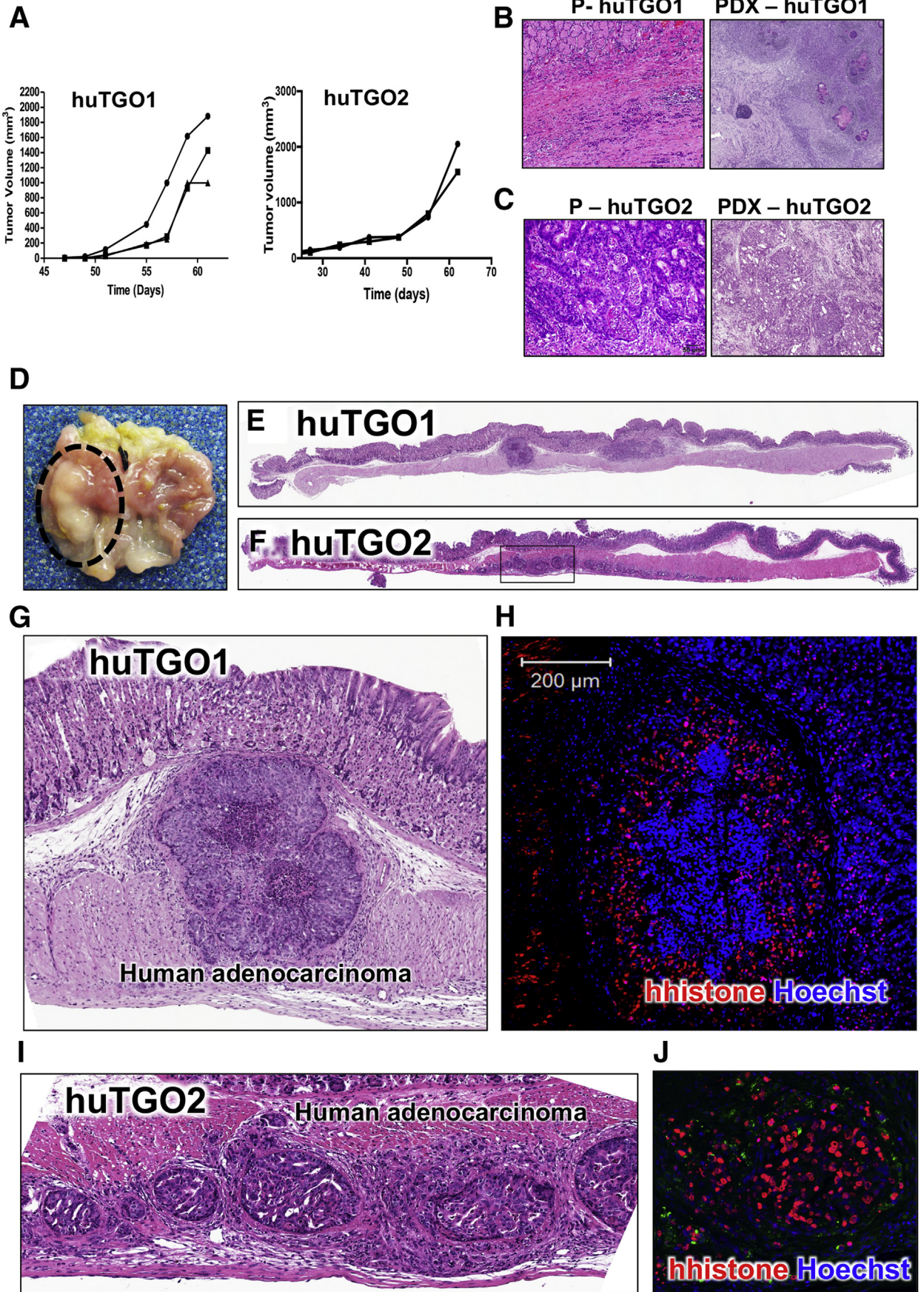
C 5-FU – huTGO6

log(inhibitor) vs. normalized response	5FU	5FU + HER2I
LogIC50	1.669 ± 0.09	1.12 ± 0.06
IC50	46.66 ± 0.09	13.17 ± 0.06
95% CI (profile likelihood)		
LogIC50	1.465 to 1.857	0.9701 to 1.269
IC50	29.18 to 71.9	9.336 to 18.59

Figure 10. IC50 values for huTGO6 dose-response curves. IC50 values for tumor-derived gastric organoids (huTGO) treated with (A) epirubicin with or without HER2I, (B) oxaliplatin with or without HER2I, or (C) 5-FU with or without HER2I. CI, confidence interval.

that human-derived cancer organoids represent typical characteristics and altered pathways of gastric cancer. Although the report also documents that gastric cancer organoids derived from individual patients exhibit divergent drug responses, this study fails to address the original patient's tumor responses to treatment. Although a limitation of our current study is the small sample size, we report a potential correlation between organoid responses to chemotherapy with the patient's own tumor response from which the cultures were derived. In support of this, huTGO7

organoid line was highly chemosensitive to the combination treatment of epirubicin, oxaliplatin, and 5-FU (Figure 5A). Importantly, huTGO7 was derived from a patient who was diagnosed with a complete response to chemotherapy (Table 1). In contrast, huTGO4 responded partially to the combination in vitro treatment of the organoids (Figure 5A); however, this patient did not respond to chemotherapy treatment (Table 1). One potential explanation for these data is the absence of the patient's immune component in the culture system. Immune dysregulation may contribute



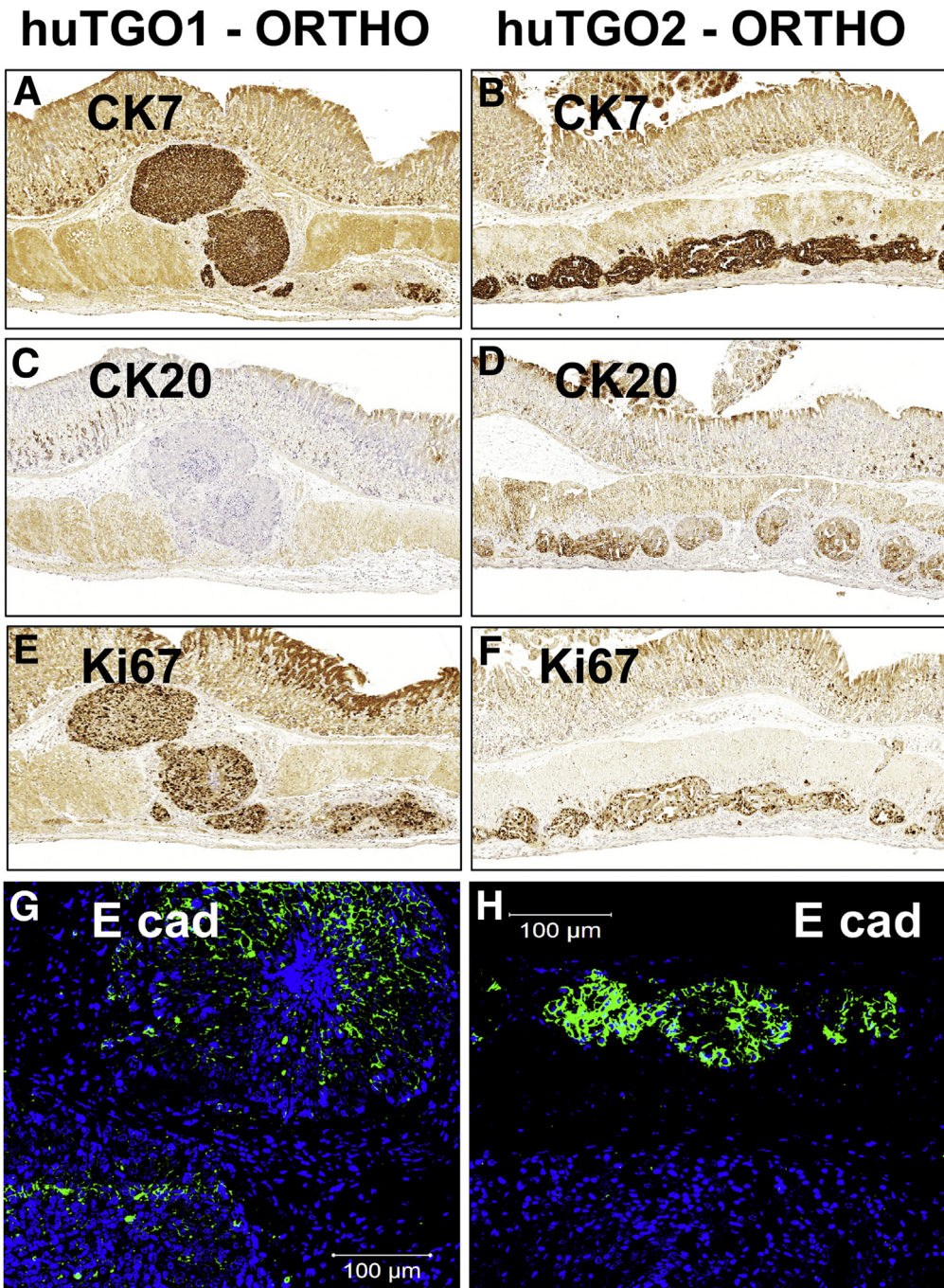


Figure 12. Engraftment and immunostaining of adenocarcinoma arising from orthotopically transplanted patient-derived gastric cancer organoids. Immunohistochemical evaluation of CK7 in orthotopic (A) huTGO1 or (B) huTGO2 transplanted mouse stomachs. Immunohistochemical analysis of CK20 in orthotopic (C) huTGO1 or (D) huTGO2 transplanted mouse stomachs. Immunohistochemistry of Ki67 expression in orthotopic (E) huTGO1 or (F) huTGO2 transplanted mouse stomachs. Immunofluorescence of E-cadherin expression (E cad, green) in orthotopic (G) huTGO1 or (H) huTGO2 transplanted mouse stomachs.

to tumor progression in gastric cancer. For example, it has been shown that the infiltration of myeloid-derived suppressor cells contributes not only to the suppression of

T-cell activation but also the impairment of the efficacy of cancer immunotherapy.^{24,25} Thus, we may speculate that if the patient from whom huTGO4 was derived exhibited high

Figure 11. (See previous page). Analysis of patient-derived gastric cancer organoid xenografts and orthotopic transplants. (A) Tumor volume measured over time of patient-derived xenografts (PDX). H&E staining of patient tumor tissue and patient-derived xenografts from (B) P1; PDX-huTGO1 and (C) P2; PDX-huTGO2. (D) Gross morphology of gastric tumor 30 days after orthotopic transplantation of patient-derived gastric cancer organoids in NSG mice. H&E staining of NSG mouse stomachs orthotopically transplanted with (E) huTGO1 and (F) huTGO2 30 days after injection. High-power magnification of human adenocarcinoma within submucosa of mice transplanted with (G) huTGO1 and (I) huTGO2. Immunofluorescence staining of human histone (red) and nuclear staining (Hoescht, blue) in NSG mouse stomachs orthotopically transplanted with (H) huTGO1 or (J) huTGO2.

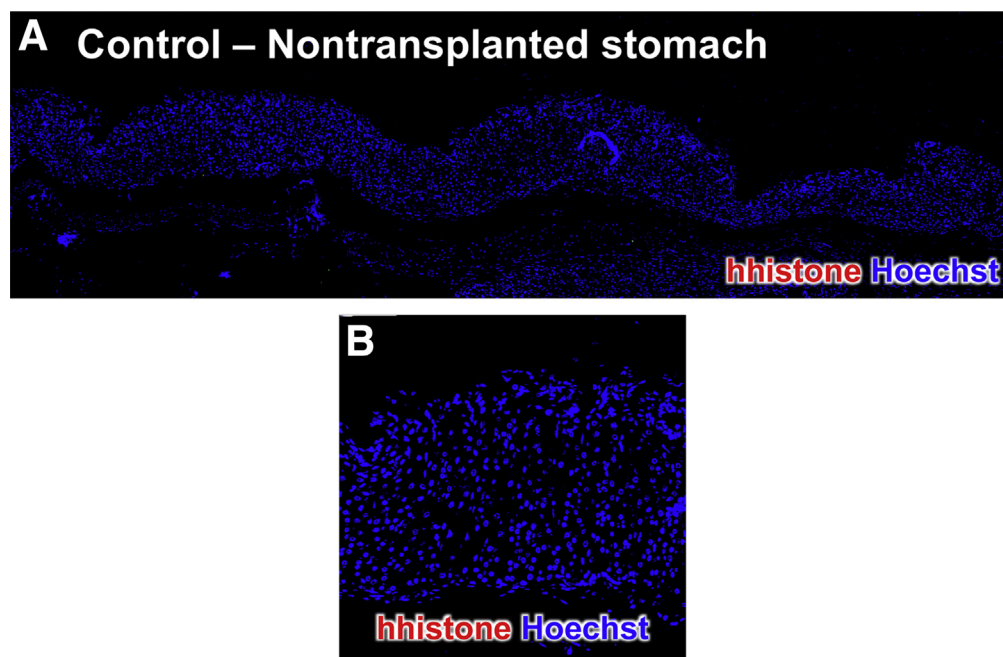


Figure 13. Human histone immunofluorescence of nontransplanted mouse stomach. (A) Immunofluorescence of nontransplanted mouse stomach using an antibody specific for human histone (red) and Hoechst (blue). (B) Higher magnification is shown.

infiltrating myeloid-derived suppressor cells, then the patient's tumor response would be poor. However, in vitro in the absence of these immunosuppressive myeloid-derived suppressor cells and cytotoxic T lymphocytes, it may be expected that the huTGO4 cultures would exhibit increased chemosensitivity. Thus, our future studies will include co-culturing patient-derived immune cells and tumor organoids to investigate the potential effect of immune-tumor cell cross talk on treatment response. Importantly, our plans also entail using a larger patient sample size to truly predict patient outcome based on an organoid-based response to chemotherapy.

Our data suggest that gastric cancer organoids may be used to help predict patient response to targeted therapies such as HER2 inhibition. Expression of HER2 within organoid cultures (huTGO1 and huTGO2) that were 2 of the resistant lines to chemotherapy treatment was sensitized to these chemotherapeutic agents with HER2 inhibitor pretreatment. HER2 overexpression is becoming recognized as a frequent molecular abnormality in gastric cancer.²⁶ Amplification of the HER2 gene was first discovered in breast cancer and is significantly associated with worse prognosis.²⁷ With the recent introduction of HER2 molecular targeted therapy for patients with metastatic gastric cancer, determination of HER2 status is crucial to select patients who may benefit from this treatment. However, HER2 testing in gastric cancer differs from testing in breast cancer because of inherent differences in tumor biology, tumor heterogeneity of HER2 expression, and incomplete membrane staining that are commonly observed in gastric cancers.⁶ The organoid culture system may provide a reliable method for identifying HER2-positive patients because the culture is designed to select for the cancer

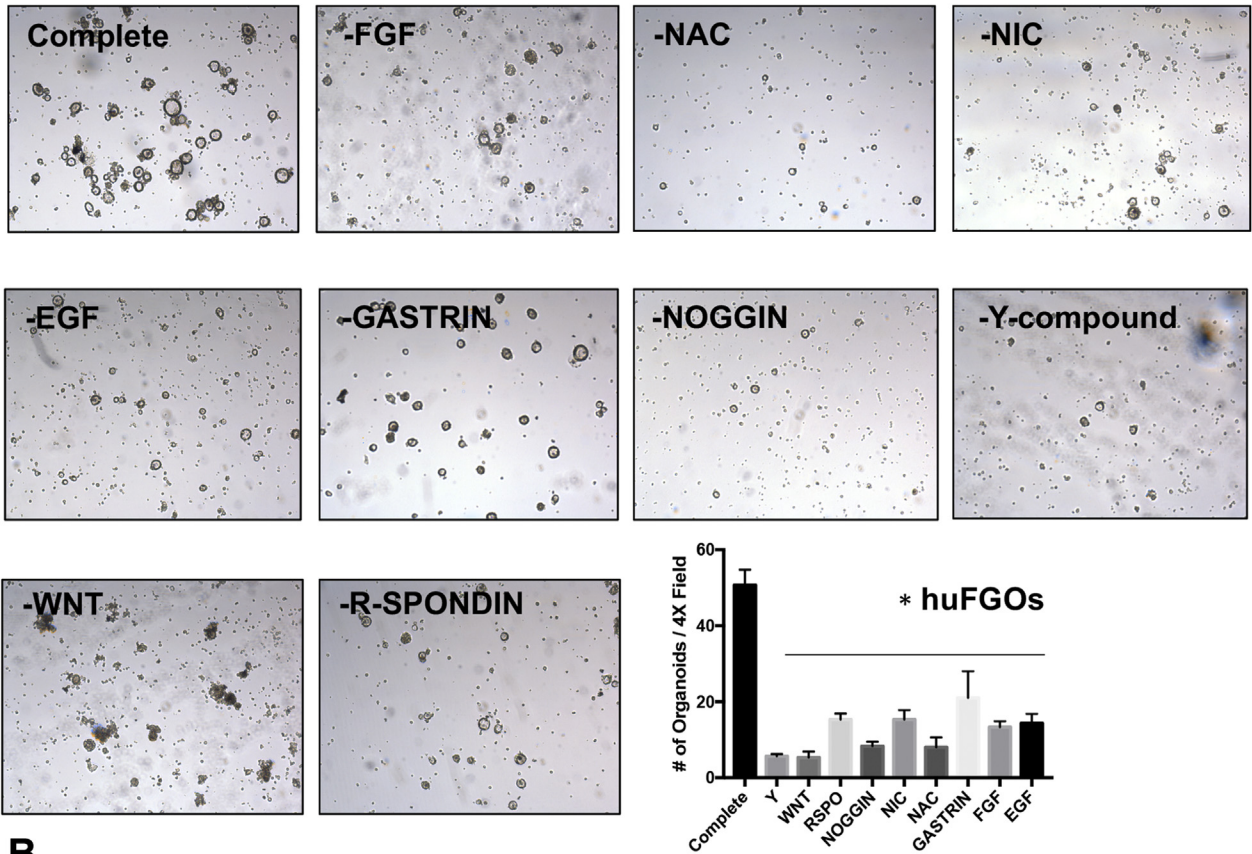
stem cells. Treating organoids alongside the patients from whom the cultures were derived will ultimately test their usefulness to predict individual therapy response and patient outcome.

Materials and Methods

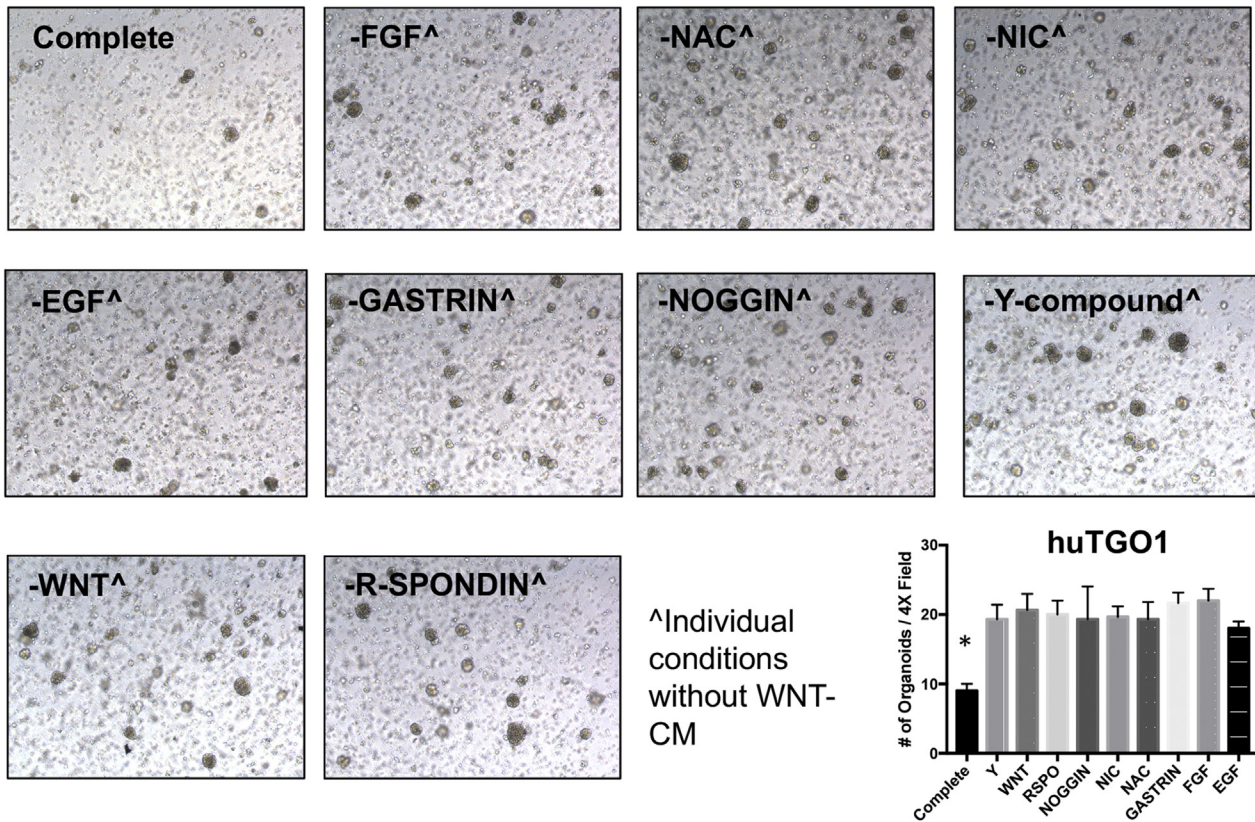
Generating Human Fundic Gastric Organoids

Human fundus was collected from sleeve gastrectomies (IRB protocol number: 2015-5537, University of Cincinnati and 2014-0427, Cincinnati Children's Hospital Medical Center), and gastric glands were generated as previously described.^{28,29} Briefly, epithelial tissue was separated from the muscle layer, cut into small fragments, and washed in Dulbecco phosphate-buffered saline (DPBS) without $\text{Ca}^{2+}/\text{Mg}^{2+}$. Tissue fragments were placed in a buffer containing collagenase (1 mg/mL) from *Clostridium histolyticum* and bovine serum albumin (2 mg/mL) for 30 minutes at 37°C. Gastric glands were suspended in 50 μL Matrigel (Thermo Fisher Scientific, Waltham, MA) and cultured in freshly generated human gastric organoid media (DMEM/F12 (Thermo Fisher Scientific), HEPES (10 mmol/L), 1X L-glutamine (Thermo Fisher Scientific), 1X Pen/Strep, 1X N2 (Thermo Fisher Scientific), 1X B27 (Thermo Fisher Scientific), N-acetylcysteine (1 mmol/L; Sigma-Aldrich, St Louis, MO), nicotinamide (10 mmol/L; Sigma-Aldrich), epidermal growth factor (50 ng/mL; Pepro-Tech, Rocky Hill, NJ), noggin (100 ng/mL; PeproTech), R-spondin conditioned media, wnt conditioned media, FGF10 (200 ng/mL; PeproTech), gastrin (1 nmol/L; Tocris Bioscience, Bristol, United Kingdom), Y-27632 (10 $\mu\text{mol/L}$; Sigma-Aldrich), 1X amphotericin B/gentamicin, 1X kanamycin). Organoids were harvested after 4–7 days of growth.

A



B



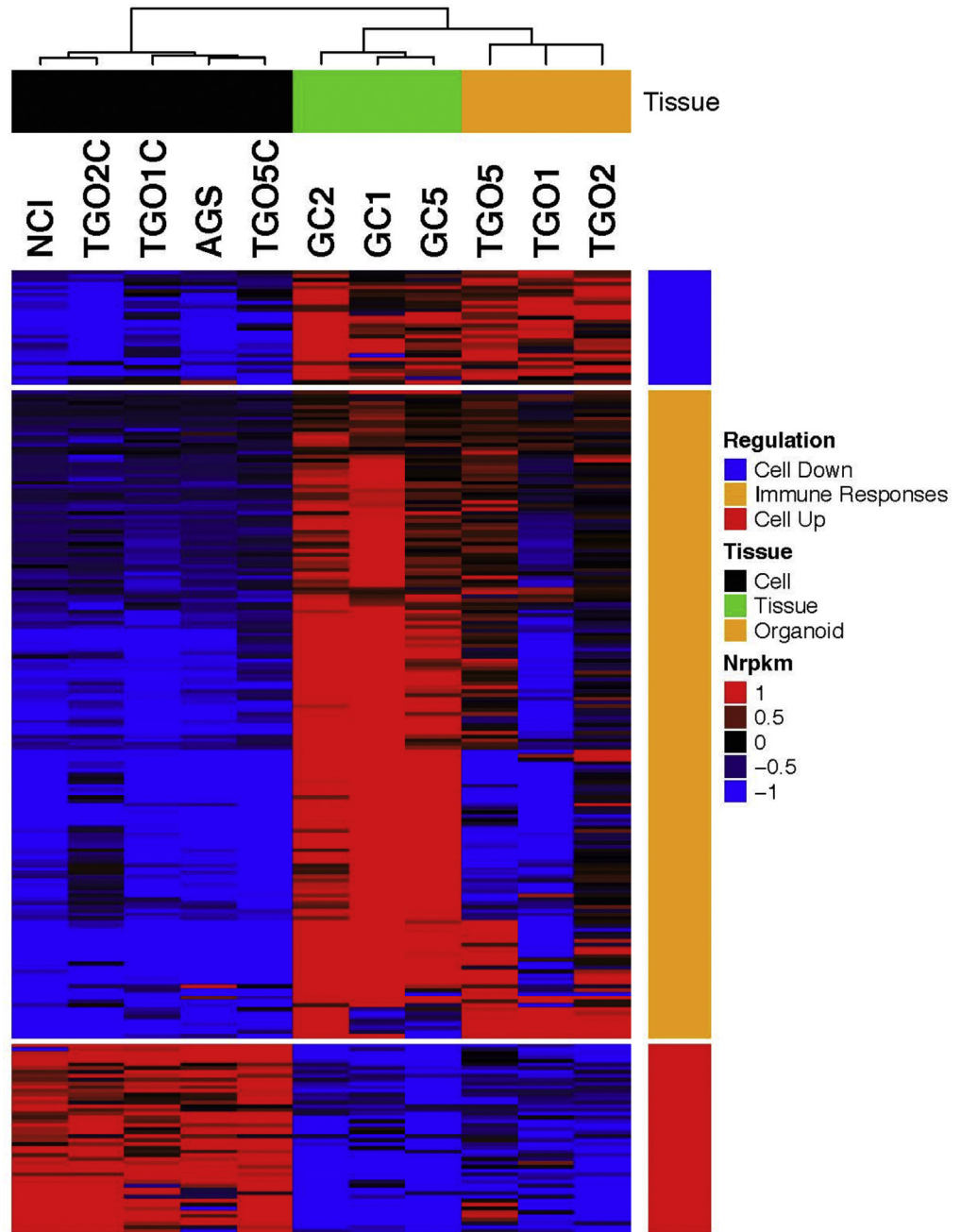


Figure 15. RNA sequencing analysis of gastric cancer patient tissue (GC), organoid (TGOs), and cell lines (AGS, NCI, or TGOC). RNA sequencing analysis of gastric cancer cell lines (NCI, AGS), organoid-derived gastric cancer cell lines (TGO1C, TGO2C, TGO5C), patient tissue (GC1, GC2, GC5), and patient-derived gastric cancer organoids (TGO1, TGO2, TGO5).

Organoids Derived From Gastric Cancer Tissue

Tumor tissue was obtained from patients undergoing surgical resection for gastric cancer (IRB protocol number: 2015-5537, University of Cincinnati and H-35094, Baylor College of Medicine). Tumor organoids were generated as previously described.³⁰ Briefly, tumor tissue was washed well in DPBS without Ca^{2+} and Mg^{2+} supplemented with

antibiotics and minced into small pieces. Tumor fragments were placed in pre-warmed stripping buffer: Hank's balanced salt solution, ethylenediamine tetraacetic acid (5 mmol/L), HEPES (25 mmol/L), 10% fetal calf serum. Fragments were incubated for 10 minutes in a shaking incubator at 37°C. The fragments were supplied fresh stripping buffer and incubated for an additional 5 minutes

Figure 14. (See previous page). Growth factor independent growth of gastric cancer organoids. Light micrographs of organoids derived from (A) normal (huFGOs) or (B) gastric cancer (huTGO1) organoid line in various growth factor conditions. Quantification of number of organoids per 4× field is shown for both huFGOs and huTGO1. * $P < .05$ compared with complete media condition, $n = 3$ individual organoid lines.

Table 2. Immune Response GO Categories Identified in the Enrichment Analysis of the Genes in the Immune Responses Cluster in Figure 15

GO	GO names	Differentially expressed	In GO category	False discovery rate
GO:0006955	Immune response	46	771	4.69*10 ⁻¹⁰
GO:0002682	Regulation of immune system process	42	653	4.69*10 ⁻¹⁰
GO:0050776	Regulation of immune response	31	408	1.00*10 ⁻⁸
GO:0044421	Extracellular region part	42	739	1.40*10 ⁻⁸
GO:0050778	Positive regulation of immune response	24	281	1.37*10 ⁻⁷
GO:0002429	Immune response-activating cell surface receptor signaling pathway	16	120	2.36*10 ⁻⁷
GO:0002504	Antigen processing and presentation of peptide or polysaccharide antigen via MHC class II	8	19	3.41*10 ⁻⁷
GO:0002768	Immune response-regulating cell surface receptor signaling pathway	16	125	3.41*10 ⁻⁷
GO:0042613	MHC class II protein complex	7	13	3.92*10 ⁻⁷
GO:0001775	Cell activation	34	590	4.39*10 ⁻⁷

in a shaking incubator at 37°C. The tissue fragments were washed with Hank's balanced salt solution twice, and pre-warmed incubation buffer (RPMI supplemented with collagenase [1.5 mg/mL] and hyaluronidase [20 µg/mL]) was added to the fragments and incubated at 37°C for 30 minutes in a shaking incubator. The digest was diluted with 20 mL DPBS without Ca²⁺ and Mg²⁺ supplemented with antibiotics and filtered through a 70-µm filter. The cells were centrifuged at 1200 rpm for 5 minutes and embedded into Matrigel supplemented with gastric growth medium as described above.

Orthotopic Transplantation of Gastric Organoids

All mouse studies were approved by the University of Cincinnati Institutional Animal Care and Use Committee that maintains an American Association of Assessment and Accreditation of Laboratory Animal Care facility. Orthotopic transplantation of gastric organoids was performed in NOD scid gamma (NSG) mice according to a previously published protocol.²⁹ Briefly, an acetic acid injury was induced. After injury, approximately 500 organoids were resuspended in 1:1 Matrigel/PBS solution and injected within the submucosa. Stomach tissues were collected 14, 30, and 60 days after transplantation.

Mouse Xenograft Assay

Xenograft assays were performed by injecting approximately 500 organoids subcutaneously in the right flank of NSG mice. Tumor dimensions were measured every 3–7 days.

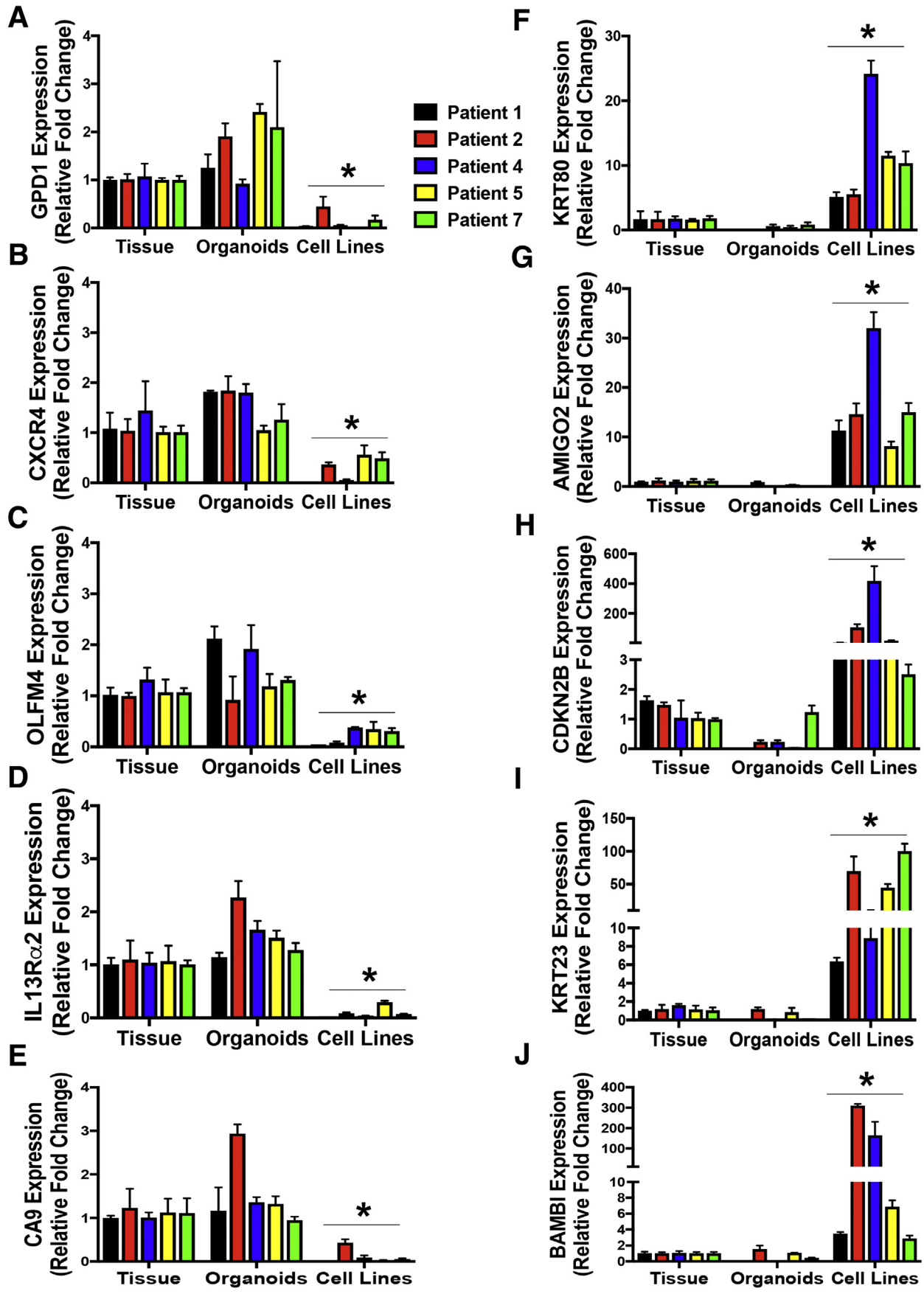
Immunofluorescence

Stomach tissues were collected and fixed in 4% paraformaldehyde for 16 hours, and longitudinal sections were paraffin-embedded and sectioned at 5 µm. Tissue slides were deparaffinized and boiled in antigen citrate buffer (Vector Laboratories, Burlingame, CA; H3300) for 10 minutes. Sections were then blocked with 20% donkey serum for 20 minutes and immunostained with primary

antibodies overnight at 4°C, followed by incubation with secondary antibodies for 1 hour. Whole mount staining of gastric organoids derived from fresh tissue was performed as previously described.²⁸ Briefly, organoids were fixed in 3.7% formaldehyde for 15 minutes at room temperature. Organoids were permeabilized with 0.5% Triton X-100 for 20 minutes at room temperature. Organoids were incubated with primary antibody overnight and washed in PBS containing 0.01% Triton-X 100. Secondary antibody incubation was also performed overnight in gastric organoids and subsequently immunostained for cell nuclei using 10 µg/mL Hoechst. The following primary antibodies and dilutions were used: 1:100 human-specific rabbit anti histone (Abcam, Cambridge, United Kingdom; ab125027), 1:100 rabbit anti-HER2 (Novus Biologicals, Littleton, CO; NBP1-84584), and 1:400 goat anti-Ecad (R&D Systems, Minneapolis, MN; AF648). For measurement of proliferation, EdU solution was added to the organoid medium of huTGOs or huFGOs for 1-hour uptake. EdU staining was performed by using the Click-iT Alexa Fluor 594 Imaging Kit, according to the manufacturer's instructions (Life Technologies, Carlsbad, CA). Coverslips were mounted onto slides with Vectashield Mounting Medium (Vector Laboratories; H-1400), and slides and whole mount organoids were imaged on a Zeiss LSM710 LIVE (Carl Zeiss AG, Oberkochen, Germany) duo confocal microscope.

Immunohistochemistry

Stomach sections spanning both the fundic and antral regions collected from mice orthotopically transplanted with huTGOs were fixed for 16 hours in 4% paraformaldehyde, paraffin embedded, and sectioned at 5 µmol/L. Prepared slides were deparaffinized with antigen retrieval performed by submerging in boiling solution (1:100 dilution Antigen Unmasking Solution in dH₂O; Vector Laboratories; H-3300) for 10 minutes, followed by 20 minutes at room temperature. Sections were then blocked and immunostained with 1:100 CK7 (Novus Biologicals; NBP2-44814), 1:100 CK20 (Novus Biologicals; NBP1-85599), or 1:400



Ki67 (Thermo Fisher Scientific; RM-9106-SO). Slides were incubated with biotinylated anti-mouse or anti-rabbit secondary antibodies for 30 minutes, followed by additional 30-minute incubation with ABC reagent (Vectastain ABC kit; Vector Laboratories). Color was developed with 3,3'-diaminobenzidine (DAB) using the DAB Substrate Kit (Vector Laboratories), and slides were then counterstained with hematoxylin (Fisher Scientific Company, Kalamazoo, MI). Immunohistochemical slides were dehydrated and mounted using Permount (Fisher Scientific), and images were viewed and captured under light microscopy (Olympus BX60 with Diagnostic Instruments "Spot" Camera; Tokyo, Japan).

Drug Assay in Tumor-Derived Organoids

Organoids were grown in 96-well plates and treated with epirubicin, oxaliplatin, or 5-FU (EOX) (Selleckchem, Houston, TX) at concentrations of 0, 0.5, 1, 5, 10, 50, 100, and 200 $\mu\text{mol/L}$ for 48 hours. In a separate series of experiments, organoids were pretreated with HER2 inhibitor Mubritinib (Sigma-Aldrich) at concentrations of 0, 0.5, 1, 5, 10, 50, 100, and 200 $\mu\text{mol/L}$ for 2 hours before epirubicin, oxaliplatin, or 5-FU treatment at the calculated IC50 for each drug for an additional 48 hours. After 48 hours, organoid proliferation was measured by using MTS Assay (Promega 93582; Madison, WI). Dose-response curves were calculated on the basis of the absorbance readings collected from the MTS assay relative to drug concentrations. Absorbance was normalized to the vehicle controls, and drug concentrations were converted to logarithms by using GraphPad Prism (GraphPad Software, San Diego, CA).

In a separate series of experiments, huTGO or huFGO lines were grown in a 48-well plate and treated with a combination of epirubicin/oxaliplatin/5-FU at IC50 concentrations calculated for each organoid line. Organoids were then dissociated to single cells by using Accutase for 10–15 minutes at 37°C at 0, 24, 48, 72, and 96 hours after drug treatment. Organoids treated with vehicle were harvested at the same time points. Cell viability was then assayed by flow cytometry using the LIVE/DEAD Viability/Cytotoxicity Kit (ThermoFisher Scientific; L3224). The % dead cells was calculated on the basis of the ability of ethidium homodimer-1 (ex/em approximately 495/635 nm) to enter the cells with damaged membranes. All calculations were normalized to the number % live/dead cells in vehicle controls. Samples were run on the CANTO 3 and analyzed by FlowJo software.

RNA Sequencing

RNA was isolated from patient tumor tissue, gastric organoids using TRIzol (Molecular Research Center Inc, Cincinnati, OH) according to the manufacturer's instructions. RNA-seq data were aligned to the reference human genome (hg19), and expression levels of all genes were quantified by

using the standard Bioconductor workflow.³¹ The differential expression analysis between sample types was performed on the basis of the negative-binomial statistical model of read counts as implemented in the *DESeq* Bioconductor package.^{32,33} The differential expression analysis between sample types was performed on the basis of the negative-binomial statistical model of read counts as implemented in the *edgeR* Bioconductor package.³⁴ A two-factor generalized linear model was used to identify genes differentially expressed between 2 groups of samples, TGO and cancer tissues samples vs two-dimensional cultures, adjusted for the patient effect. The comparison was made. False discovery rates were calculated,³³ and genes with false discovery rates <0.1 were considered statistically significant. Cluster analysis of differentially expressed genes was performed by using Bayesian infinite mixture model-based clustering³⁵ of the normalized log-2 rpkm gene expression profiles after adjusting for the patient effect. The enrichment analysis of the clusters of differentially expressed genes was performed by using the CLEAN package.³⁶

Quantitative Real-Time Polymerase Chain Reaction

Total RNA was isolated from tissue, organoids, or cell lines by using TRIzol according to manufacturer's protocol (Life Technologies). The High Capacity cDNA Reverse Transcription Kit (Applied Biosystems, Foster City, CA) was used for cDNA synthesis of RNA following the recommended protocol. For each sample, 60 ng RNA was reverse transcribed to yield approximately 2 μg total cDNA that was then used for the real-time polymerase chain reaction. Pre-designed real-time polymerase chain reaction assays were purchased for the following genes (Thermo Fisher, Applied Biosystems): GAPDH (Hs02786624_g1), CXCR4 (Hs00607978_s1), GPD1 (Hs01100039_m1), CA9 (Hs00154208_m1), IL13RA2 (Hs00152924_m1), OLFM4 (Hs00197437), KRT80 (Hs01372365_m1), AMIGO2 (Hs05001325_s1), CDKN2B (Hs00793225_m1), KRT23 (Hs00210096_m1), BAMBI (Hs03044164_m1). Polymerase chain reaction amplifications were performed in a total volume of 20 μL containing 20X TaqMan Expression Assay primers, 2X TaqMan Universal Master Mix (Applied Biosystems; TaqMan Gene Expression Systems), and cDNA template. Each polymerase chain reaction amplification was performed in duplicate wells in a StepOne Real-Time PCR System (Applied Biosystems) by using the following conditions: 50°C 2 minutes, 95°C 10 minutes, 95°C 15 seconds (denature) and 60°C 1 minute (anneal/extend) for 40 cycles. Fold change was calculated as the following: $(C_t - C_{t \text{ high}}) = n_{\text{target}} 2^{n_{\text{target}}} / 2^{n_{\text{HPRT}}} = \text{fold change}$ where C_t = threshold cycle. The results were expressed as average fold change in gene expression relative to control, with GAPDH used as an internal control according to Livak and Schmittgen.³⁷

Figure 16. (See previous page). Validation of RNA sequencing data. Quantitative real-time polymerase chain reaction using RNA collected from gastric cancer tissue (GC), huTGOs, cell lines derived from huTGOs (huTGOC), and AGS and NCI-N87 (NCI) cell lines for the expression of (A) GPD1, (B) CXCR4, (C) OLFM4, (D) IL13R α 2, (E) CA9, (F) KRT80, (G) AMIGO2, (H) CDKN2B, (I) KRT23, and (J) BAMBI. * $P < .05$ compared with GC samples, $n = 3$ assays per sample.

Statistical Analyses

The significance of the results was tested by two-way analysis of variance or Student *t* test by using commercially available software (GraphPad Prism). A *P* value <.05 was considered significant.

References

- Ahmad SA, Xia BT, Bailey CE, Abbott DE, Helmink BA, Daly MC, Thota R, Schlegel C, Winer LK, Ahmad SA, Al Humaidi AH, Parikh AA. An update on gastric cancer. *Curr Probl Surg* 2016;53:449–490.
- Neugut AI, Hayek M, Howe G. Epidemiology of gastric cancer. *Semin Oncol* 1996;23:281–291.
- Gunturu KS, Woo Y, Beaubier N, Remotti HE, Saif MW. Gastric cancer and trastuzumab: first biologic therapy in gastric cancer. *Ther Adv Med Oncol* 2013; 5:143–151.
- Manion E, Hornick JL, Lester SC, Brock JE. A comparison of equivocal immunohistochemical results with anti-HER2/neu antibodies A0485 and SP3 with corresponding FISH results in routine clinical practice. *Am J Clin Pathol* 2011;135:845–851.
- Yano T, Doi T, Ohtsu A, Boku N, Hashizume K, Nakanishi M, Ochiai A. Comparison of HER2 gene amplification assessed by fluorescence in situ hybridization and HER2 protein expression assessed by immunohistochemistry in gastric cancer. *Oncol Rep* 2006;15:65–71.
- Abrahamo-Machado LF, Jacome AA, Wohnrath DR, dos Santos JS, Carneseca EC, Fregnani JH, Scapulatempo-Neto C. HER2 in gastric cancer: comparative analysis of three different antibodies using whole-tissue sections and tissue microarrays. *World J Gastroenterol* 2013; 19:6438–6446.
- Domcke S, Sinha R, Levine DA, Sander C, Schultz N. Evaluating cell lines as tumour models by comparison of genomic profiles. *Nat Commun* 2013;4:2126.
- Ertel A, Verghese A, Byers SW, Ochs M, Tozeren A. Pathway-specific differences between tumor cell lines and normal and tumor tissue cells. *Mol Cancer* 2006; 5:55.
- Gillet JP, Calcagno AM, Varma S, Marino M, Green LJ, Vora MI, Patel C, Orina JN, Eliseeva TA, Singal V, Padmanabhan R, Davidson B, Ganapathi R, Sood AK, Rueda BR, Ambudkar SV, Gottesman MM. Redefining the relevance of established cancer cell lines to the study of mechanisms of clinical anti-cancer drug resistance. *Proc Natl Acad Sci U S A* 2011;108:18708–18713.
- Sandberg R, Ernberg I. Assessment of tumor characteristic gene expression in cell lines using a tissue similarity index (TSI). *Proc Natl Acad Sci U S A* 2005; 102:2052–2057.
- Stein WD, Bates SE, Fojo T. Intractable cancers: the many faces of multidrug resistance and the many targets it presents for therapeutic attack. *Curr Drug Targets* 2004;5:333–346.
- Bianchini G, Gianni L. The immune system and response to HER2-targeted treatment in breast cancer. *Lancet Oncol* 2014;15:e58–e68.
- Ahmadzadeh M, Johnson LA, Heemskerk B, Wunderlich JR, Dudley ME, White DE, Rosenberg SA. Tumor antigen-specific CD8 T cells infiltrating the tumor express high levels of PD-1 and are functionally impaired. *Blood* 2009;114:1537–1544.
- Chen Z, Chen X, Zhou E, Chen G, Qian K, Wu X, Miao X, Tang Z. Intratumoral CD8(+) cytotoxic lymphocyte is a favorable prognostic marker in node-negative breast cancer. *PLoS One* 2014;9:e95475.
- Reissfelder C, Stamova S, Gossmann C, Braun M, Bonertz A, Walliczek U, Grimm M, Rahbari NN, Koch M, Saadati M, Benner A, Buchler MW, Jager D, Halama N, Khazaie K, Weitz J, Beckhove P. Tumor-specific cytotoxic T lymphocyte activity determines colorectal cancer patient prognosis. *J Clin Invest* 2015;125:739–751.
- Wu C, Zhu Y, Jiang J, Zhao J, Zhang XG, Xu N. Immunohistochemical localization of programmed death-1 ligand-1 (PD-L1) in gastric carcinoma and its clinical significance. *Acta Histochem* 2006;108:19–24.
- Abdel-Rahman O. PD-L1 expression and outcome of advanced melanoma patients treated with anti-PD-1/PD-L1 agents: a meta-analysis. *Immunotherapy* 2016; 8:1081–1089.
- Abdel-Rahman O. Correlation between PD-L1 expression and outcome of NSCLC patients treated with anti-PD-1/PD-L1 agents: a meta-analysis. *Crit Rev Oncol Hematol* 2016;101:75–85.
- Abdel-Rahman O. Immune checkpoints aberrations and gastric cancer: assessment of prognostic value and evaluation of therapeutic potentials. *Crit Rev Oncol Hematol* 2016;97:65–71.
- Takami H, Sentani K, Matsuda M, Oue N, Sakamoto N, Yasui W. Cytokeratin expression profiling in gastric carcinoma: clinicopathologic significance and comparison with tumor-associated molecules. *Pathobiology* 2012; 79:154–161.
- Chu PG, Weiss LM. Keratin expression in human tissues and neoplasms. *Histopathology* 2002;40: 403–439.
- Busuttill RA, Liu DS, Di Costanzo N, Schroder J, Mitchell C, Boussioutas A. An orthotopic mouse model of gastric cancer invasion and metastasis. *Sci Rep* 2018; 8:825.
- Seidlitz T, Merker SR, Rothe A, Zakrzewski F, von Neubeck C, Grutzmann K, Sommer U, Schweitzer C, Scholch S, Uhlemann H, Gaebler AM, Werner K, Krause M, Baretton GB, Welsch T, Koo BK, Aust DE, Klink B, Weitz J, Stange DE. Human gastric cancer modelling using organoids. *Gut* 2018 [Epub ahead of print].
- Wang L, Chang EW, Wong SC, Ong SM, Chong DQ, Ling KL. Increased myeloid-derived suppressor cells in gastric cancer correlate with cancer stage and plasma S100A8/A9 proinflammatory proteins. *J Immunol* 2013; 190:794–804.
- Shoji H, Tada K, Kitano S, Nishimura T, Shimada Y, Nagashima K, Aoki K, Hiraoka N, Honma Y, Iwasa S, Takashima A, Kato K, Boku N, Honda K, Yamada T, Heike Y, Hamaguchi T. The peripheral immune status of granulocytic myeloid-derived suppressor cells correlates the survival in advanced gastric cancer patients receiving

- cisplatin-based chemotherapy. *Oncotarget* 2017; 8:95083–95094.
26. Ruschoff J, Dietel M, Baretton G, Arbogast S, Walch A, Monges G, Chenard MP, Penault-Llorca F, Nagelmeier I, Schlake W, Hofler H, Kreipe HH. HER2 diagnostics in gastric cancer-guideline validation and development of standardized immunohistochemical testing. *Virchows Arch* 2010;457:299–307.
 27. Slamon DJ, Clark GM, Wong SG, Levin WJ, Ullrich A, McGuire WL. Human breast cancer: correlation of relapse and survival with amplification of the HER-2/neu oncogene. *Science* 1987;235:177–182.
 28. Bertaux-Skeirik N, Feng R, Schumacher MA, Li J, Mahe MM, Engevik AC, Javitt JE, Peek RM Jr, Ottemann K, Orian-Rousseau V, Boivin GP, Helmuth MA, Zavros Y. CD44 plays a functional role in *Helicobacter pylori*-induced epithelial cell proliferation. *PLoS Pathog* 2015;11:e1004663.
 29. Engevik AC, Feng R, Choi E, White S, Bertaux-Skeirik N, Li J, Mahe MM, Aihara E, Yang L, DiPasquale B, Oh S, Engevik KA, Giraud AS, Montrose MH, Medvedovic M, Helmuth MA, Goldenring JR, Zavros Y. The development of spasmodic polypeptide/TFF2-expressing metaplasia (SPEM) during gastric repair is absent in the aged stomach. *Cell Mol Gastroenterol Hepatol* 2016;2:605–624.
 30. Bertaux-Skeirik N, Centeno J, Gao J, Gao J, Gabre J, Zavros Y. Oncogenic transformation of human-derived gastric organoids. *Methods Mol Biol* 2016:1–9.
 31. Huber W, Carey VJ, Gentleman R, Anders S, Carlson M, Carvalho BS, Bravo HC, Davis S, Gatto L, Girke T, Gottardo R, Hahne F, Hansen KD, Irizarry RA, Lawrence M, Love MI, MacDonald J, Obenchain V, Oles AK, Pages H, Reyes A, Shannon P, Smyth GK, Tenenbaum D, Waldron L, Morgan M. Orchestrating high-throughput genomic analysis with Bioconductor. *Nat Meth* 2015;12:115–121.
 32. Anders S, Huber W. Differential expression analysis for sequence count data. *Genome Biol* 2010;11:R106.
 33. Benjamini Y, Hochberg Y. Controlling the false discovery rate: a practical and powerful approach to multiple testing. *J Roy Stat Soc B* 1995;57:289–300.
 34. Robinson MD, McCarthy DJ, Smyth GK. edgeR: a Bioconductor package for differential expression analysis of digital gene expression data. *Bioinformatics* 2010; 26:139–140.
 35. Freudenberg JM, Sivaganesan S, Wagner M, Medvedovic M. A semi-parametric Bayesian model for unsupervised differential co-expression analysis. *BMC Bioinformatics* 2010;11:234.
 36. Freudenberg JM, Joshi VK, Hu Z, Medvedovic M. CLEAN: CLustering Enrichment ANalysis. *BMC Bioinformatics* 2009;10:234.
 37. Livak K, Schmittgen T. Analysis of relative gene expression data using real-time quantitative PCR and the 2(-Delta Delta C(T)) method. *Methods* 2001;25:402–408.

Received October 5, 2017. Accepted September 10, 2018.

Correspondence

Address correspondence to: Yana Zavros, PhD, University of Cincinnati College of Medicine, Department of Pharmacology and Systems Physiology, 231 Albert B. Sabin Way, Room 4255 MSB, Cincinnati, Ohio 45267-0576. e-mail: yana.zavros@uc.edu; fax: (513) 558-3756.

Acknowledgments

The authors acknowledge the assistance of Chet Closson (Live Microscopy Core, University of Cincinnati). The authors thank Lisa McMillin (Cincinnati Children's Hospital Medical Center, Pathology Research Core) for her assistance with organoid embedding and processing; Kathy McClinchey and the McClinchey Histology Lab Inc and Glenn Doerman (Cancer Biology, Graphic Design, Illustrations, Presentations and Desktop Publishing) for helping us prepare the figures for submission. The authors acknowledge Dr Joel Gabre for his insightful conversation. Finally, the authors thank the patients who consented to donate tissue and blood for the development of the gastric organoids. Without their willingness to participate in the study, this work would not be possible.

Author contributions

N.S., J.W., J.C., L.H., J.B.: study concept and design; acquisition of data; analysis and interpretation of data; drafting of the manuscript; critical revision of the manuscript for important intellectual content; statistical analysis; technical or material support. J.C., L.M.N., J.H., M.M., N.S.: critical revision of the manuscript for important intellectual content; technical or material support. N.S., M.M., M.H., S.A.: study concept and design; analysis and interpretation of data; drafting of the manuscript; critical revision of the manuscript for important intellectual content; technical or material support. Y.Z.: study concept and design; acquisition of data; analysis and interpretation of data; drafting of the manuscript; critical revision of the manuscript for important intellectual content; statistical analysis; obtained funding; study supervision.

Conflicts of interest

The authors disclose no conflicts.

Funding

Supported by NIH (NIDDK) 2 R01 DK083402-06A1 grant, College of Medicine Bridge Funding Program (Y.Z.) and NIH 1U19AI116491-01 (Weis and J.W., Y.Z. Project Leader), and the University of Cincinnati Graduate School Dean's Fellowship and Albert J. Ryan Fellowship and 2T32GM105526-04 (N.G.S.). This project was supported in part by PHS Grant P30 DK078392 (Integrative Morphology Core) of the Digestive Diseases Research Core Center in Cincinnati.